Aalborg Universitet

Integrated demand response for a load serving entity in multi-energy market considering network constraints

Liu, Peiyun; Ding, Tao; Zou, Zhixiang; Yang, Yongheng

Integrated Demand Response for a Load Serving Entity in Multi-Energy Market Considering Network Constraints

Tao Ding[a*1], Peiyun Liu[a], Zhixiang Zou[b], Yongheng Yang[c]

[a]*State Key Laboratory of Electrical Insulation and Power Equipment, Xi'an Jiaotong University, Xi'an, 710049, China*

[b]*Chair of Power Electronics, Christian-Albrechts-University of Kiel, Kaiserstrasse 2, Kiel 24143, Germany*

[c]*Department of Energy Technology, Aalborg University, Pontoppidanstraede 101, Aalborg 9220, Denmark*

Abstract

The rapid development of an integrated energy system makes it difficult for traditional power market to adapt to the trend of multi-energy interactions. Therefore, a tri-layer multi-energy day-ahead market structure and operation mechanism, allowing the simultaneous trading of electricity, heat and natural gas, are proposed in this paper. Concentrating on the profit of the load serving entity in this market, the optimal transaction strategy based on the integrated demand response is explicitly modeled in detail. In particular, the physical constraints of the power distribution network, natural gas network and district heating network are strictly considered. To address the nonlinear and nonconvex problems in the distribution network and natural gas network, the mixed-integer second-order cone programming method and piecewise linearization process are used. Furthermore, a novel conditional value at risk approach is proposed to address the uncertain forecasted market prices, so that the risk can be mitigated. Compared with the traditional electricity market, the LSE can earn a higher profit in the proposed market, and the integrated demand response program enhances the potential of multi-energy peak load shifting. Finally, the effectiveness of the proposed method has been verified on an integrated energy system with IEEE 33-bus power system, an 11-node gas system and a 6-node heat system. A set of comparative cases verify the necessity for the IES to keep the balance between the market economy and network security operation.

Keywords: Integrated energy system; multi-energy market; load serving entity; integrated demand response

Indices and sets

t	Index of the trading period
s	Index of the energy supply
l	Index of the energy demand
P, G, H	Index of the electricity, natural gas, and heat, respectively
T	Number of trading periods
S	Index of the supply network
R	Index of the return network
$\Omega_P^{load}, \Omega_G^{load}, \Omega_H^{load}$	Set of power loads/natural gas loads/heat loads
$\Omega_P^{bus}, \Omega_G^{node}, \Omega_H^{node}$	Set of power buses/natural gas nodes/heat nodes
$\Omega_P^{s}, \Omega_G^{s}, \Omega_H^{s}$	Set of electricity/natural gas/heat sources

Ω_P^{branch}, Ω_G^{pipe}	Set of power branches/natural gas pipes
Ω_{HS}^{pipe}	Set of pipelines connected to heat sources
Ω_{HS}^{node}	Set of nodes connected to heat sources
Ω_{HL}^{pipe}	Set of pipelines connected to heat loads
Ω_{HL}^{node}	Set of nodes connected to heat loads
Ω_H^{Spipe} Ω_H^{Rpipe}	Set of supply/return pipes in DHS
Ω^{Spipe^+}, Ω^{Rpipe^+}	Set of inlets of supply/return pipes
Ω^{Spipe^-}, Ω^{Rpipe^-}	Set of outlets of supply/return pipes

Variables

Energy market

$P_{s,t}$, $G_{s,t}$, $H_{s,t}$	The amount of electricity/natural gas/heat that the LSE purchased from the wholesale market at period t
$P_{l,t}$, $G_{l,t}$, $H_{l,t}$	The amount of electricity/natural gas/heat that the LSE sold in retail market at period t
E_α, E_β	The input energy α and output energy β in an energy hub
$P_{out,t}$, $G_{out,t}$, $H_{out,t}$	The amount of electricity, natural gas and heat output of energy hub at period t
$P_{in,t}$, $G_{in,t}$, $H_{in,t}$	The amount of electricity, natural gas and heat input of an energy hub at period t
$G_{c,t}$, $P_{c,t}$	The amount of gas that can be injected from a gas/electricity storage at period t
$G_{dc,t}$, $P_{dc,t}$	The amount of gas that can be delivered from a gas/electricity storage at period t
GS_t, PS_t	The total energy reserved in a gas/ electricity storage at period t

Power system

$P_{w,t}$, $Q_{w,t}$	Net active/reactive power injection on bus w at period t
$\upsilon_{w,t}$	Voltage magnitude on bus w at period t
$I_{wz,t}$	Current magnitude from bus z to bus z at period t
$P_{b,t}$, $Q_{b,t}$	Net active/reactive power on branch b at period t

Gas system

$fp_{p,t}$	Natural gas flow of pipeline p for period t
$\pi_{n,t}$	Pressure in gas node n for period t
$\eta_{p,k}$	The k-th dummy binary variable for linearizing pipe p
$\delta_{p,k}$	The k-th dummy continuous variable for linearizing pipe p

Heat system

$\tau_{n,t}^S$, $\tau_{n,t}^R$	The mixed temperature at node n of the supply network/return network at period t
$\tau_{j,t}^S$, $\tau_{j,t}^R$	The supply/return temperature of pipe j at period t
$H_{loss,j,t}$	The heat loss of pipeline j at period t
$\tau_{j,t}^{in}$, $\tau_{j,t}^{out}$	Inlet temperature/outlet temperature of pipe j at period t

Parameters

Energy market

$\rho_{Ps,t}$, $\rho_{Gs,t}$, $\rho_{Hs,t}$	Wholesale prices of electricity, natural gas and heat at period t
$\rho_{Pl,t}$, $\rho_{Gl,t}$, $\rho_{Hl,t}$	Retail prices of electricity, natural gas and heat at period t
$P_{s,\min}$, $G_{s,\min}$, $H_{s,\min}$	The lower bound of the power/gas/heat supply s
$P_{s,\max}$, $G_{s,\max}$, $H_{s,\max}$	The upper bound of the power/gas/heat supply s
$P_{l,\min}$, $G_{l,\min}$, $H_{l,\min}$	The lower bound of the power/gas/heat load l
$P_{l,\max}$, $G_{l,\max}$, $H_{l,\max}$	The upper bound of the power/gas/heat load l
$P_{l,day}$, $G_{l,day}$, $H_{l,day}$	The amount of the power/gas/heat load demand within one day

RES_P , RES_G , RES_H	Reserve power/gas/heat of LSE
$\gamma_{\alpha\beta}$	Energy conversion coefficient from energy α to energy β
A	Multiple energy coupling matrix of an energy hub
ζ_G , ζ_P	Injection and delivery efficiency of gas /electricity t storage
GS_{min} PS_{min}	The lower bound of total energy reserved in gas/electricity storage
GS_{max} PS_{max}	The upper bound of total energy reserved in gas /electricity storage
$G_{c,min}$ $P_{c,min}$	The lower bound of energy injection in gas /electricity storage
$G_{c,max}$ $P_{c,max}$	The upper bound of energy injection in gas /electricity storage
$G_{dc,min}$ $P_{dc,min}$	The lower bound of energy injection in gas /electricity storage
$G_{dc,max}$ $P_{dc,max}$	The upper bound of energy injection in gas /electricity storage
	Power system
r_{vw} , x_{vw}	Resistance/Reactance on the branch from bus v to bus w
$\upsilon_{w,min}$, $\upsilon_{w,max}$	The minimum/maximum limits of voltage on bus w
$I_{wz,min}$, $I_{wz,max}$	The minimum/maximum limits of the current on branch from bus w to bus z
	Gas system
$fp_{p,min}$, $fp_{p,max}$	The minimum/maximum limits of the gas flow on natural gas pipeline p
$\pi_{n,min}$, $\pi_{n,max}$	The minimum/maximum limits of the gas pressure on gas node n
NPL	The number of linear segments
ϕ_p	Parameters of natural gas pipeline
γ_o	Compression ratio
B_{nk}	Node-pipe incidence matrix
C_{ns}	Node-gas supply incidence matrix
D_{nl}	Node-gas load incidence matrix
	Heat system
c	Specific heat capacity of water
$m_{j,t}^{HS}$	The constant mass flow of pipeline j connected with heat sources at period t
$m_{l,t}$	The constant mass flow of pipeline l connected with heat exchangers on the demand side at period t
$\tau_{n,min}^{S}$, $\tau_{n,max}^{S}$	The minimum/maximum limits of the supply network temperature at node n
$\tau_{n,min}^{R}$, $\tau_{n,max}^{R}$	The minimum/maximum limits of the return network temperature at node n
U_j	Transmission efficiency of heat pipeline j
l_j	The length of heat pipeline j
τ_g	Ground temperature

1. Introduction

The dual pressures of the energy crisis and environmental pollution pave the way to improve the contemporary energy structure [1]. According to the International Energy Agency [2], the global energy demand will increase by one-third from 2011 to 2035, while the world electricity demand will increase by more than two-thirds over the period 2011-2035. Facing a serious situation, the Energy Internet (EI) has been actively constructed to solve these increasing grave issues by integrating various forms of energy into a highly flexible and efficient smart grid **Error! Reference source not found.** [4]. In the context of an EI, the increasing development of energy coupling technology and equipment enhances the physical interconnection among different types of energy resources in recent years **Error! Reference source not found.**. Based on these technologies and devices, an integrated energy system (IES), an important type of EI, is developing

rapidly, which is the collection of multiple energy supplies, conversions, storages and demands **Error! Reference source not found.** [7]. One of the most important significances of building an EI is to improve the energy efficiency. Thus, it can make great sense for a mature EI system to develop a multi-energy market to allocate multiple resources efficiently through market mechanisms.

In the traditional electricity market, a double-sided market (i.e., the wholesale market and retail market) is the general model to ensure the efficient operation of the electric power industry [8]. Generators, independent systems operators (ISOs), load serving entities (LSEs), and power consumers are able to coordinate and cooperate with each other on this platform. Compared with the single-sided market, the double-sided electricity market allows the generators and loads to participate in it by offering curves and bids so that both the buyers and sellers can discover the market prices and the potential value of new business models and new technologies [9] [10]. The LSE is a key component of the electricity market because it is the medium that connects the wholesale market and retail market. Specifically, the LSEs obtain their retail customers' bids and take them into the wholesale market, in which the LSEs are able to submit bids to the ISOs [11]. Then, the ISOs gather the offers of the generators and bids of the LSEs and announce the wholesale electricity clearing prices in the day-ahead (DA) market [12]. The LSE is the price taker of its customers, and the price will be settled according to the load demand of the market [13]. The demand response (DR) is a critical and effective measure to stimulate the demand side loads to take part in the market. It can be further developed by the LSE through the incentives of price signals.

Existing studies on LSEs mainly focused on the achievement of market profits, DR programs, and competitive mechanisms in the electricity market. In [14], a DR program based on the electricity load classification according to the elasticity was introduced to maximize the profit of the LSE. It was concluded that the classified loads according to the elasticity difference participating in the power market could provide a strong incentive for electricity consumption, and therefore, the profit of the LSE would increase. In [15] and [16], a coupon-based DR strategy for the LSE was developed to induce the flexibility of electricity customers and then increased the profit of the LSE. The model in [16] considered the influence of wind power uncertainty, which was suitable for a power system with increasing penetration of wind power generation. The LSE day-ahead (DA) scheduling optimization framework was proposed in [17] and [18] based on load specifications. The optimal nodal hourly prices were determined by taking into account the power distribution network constraints. The results in [17] proved that the nodal hourly price could encourage the loads to change their demand pattern to reduce their electricity bill. Reference [18] concluded that the DR program through a price-responsive scheme was beneficial to lower the costs of the LSE and further improved the economic benefits of the electricity market. Reference [19] focused on the interaction mechanisms between a distribution company and the demand response aggregators, which was the same role as the LSE. It formulated a bargaining cooperative framework based on the Nash bargaining theory, and the model can facilitate cooperation and increase social welfare effectively. In [20], a Stackelberg game between the utility companies and end-users was developed to optimize the price setting and the end-users' power consumption. This strategy could ensure the reliability and dependability of the power grid. Reference [21] analyzed the nonlinear behavior of residential consumers, and in [22] a nonlinear incentive-based DR model in power market is built further. Reference [23] investigated price-controlled energy management problem of the end users to minimize overall cost of a generation company. The simulation results prove that cooperation of the residential customers in the unit commitment problem can be beneficial in decreasing cost and greenhouse gas emissions of the thermal power plants. Taking reliability-driven and market-driven measures of demand response into consideration, reference [24] proposed a model of risk-cost-based unit commitment (UC) problem mixed with demand-side resources (DSRs) to achieve overall minimum cost of system.

Currently, in addition to electricity, multiple energy conversion has become an inevitable trend, mainly including electricity-heat coupling and electricity-natural gas coupling. Based on the combined heating and power (CHP), detailed research on the optimal dispatch strategy of integrated heat and power systems was presented in [25]-[29]. In these papers, the CHP model and heat network constraints were considered, and the simulation results indicated that it was much more flexible and efficient for the integrated system to operate jointly. Reference [25] introduced the temperature dynamics and heat loss model of a district heat network, which accurately expressed the temperature changes in water pipelines. In [26], a model of a large-scale IES was presented, and the MGSO-ACL algorithm was used in the optimal power dispatch to obtain superior Pareto-optimal solutions in terms of convergence and diversity. In [27], to optimize the total operation cost of the IES, a dispatch strategy for a system considering CCHP and wind power was proposed. Several studies have focused on the electricity-gas system. Reference [30] focused on the interaction between the electricity grid and natural gas network on the residential demand side. The simulation results verified the advancement of a large number of small-scale generators for localized load balancing of the integrated system. A set of nonlinear and nonconvex equations in the natural gas system increases the complexity and difficulty of energy flow model in IES. In [31], the steady-state energy flow of an integrated natural gas and electric power system was solved by the Newton-Raphson method. In [32], the second-order cone relaxation was used in the natural gas system model to address the nonconvex problem in the original model. In [33], piecewise linear functions were adopted as the linearization of the general flow equation in both dynamic and steady-state conditions. Several case studies were compared to prove the superiority of the piecewise MILP model in terms of the calculation speed and accuracy.

In addition, an energy hub (EH), centrally equipped with a variety of energy conversion devices, made it possible to integrate heat, natural gas, electricity and other types of energy. From a system perspective, an EH gathers the multi-energy input, conversion, output, and storage in a functional unit [34]. Therefore, the EH has been studied in many works along with the IES. The EH in reference [35] comprised distribution generation, DR loads and storage, and the simulation results verified the effectiveness on reduce energy usage costs. Reference [36] built a robust optimization model of EH considering energy flow in IES, i.e. electricity, heat and gas. The proposed model was based on two-stage iterative modelling that involves Mixed Integer Linear Programming (MILP) and linear approximations of the nonlinear network equations. Reference [37] proposed a smart energy hub energy management model considering electricity and natural gas network, and integrated demand side management game in a cloud computing framework is addressed. Reference [38][35] and [39] built a residential energy hub management system, and the former proposed an optimal control model for major residential multi-energy loads and storage in real-time frame to achieve total energy cost reduction for loads, while the latter used a probabilistic optimization approach to model the uncertainty of residential loads in EH. Reference [40] also presented an optimal probabilistic scheduling model of EH operation to solve the loads and price uncertainties. Reference [41] proposed an EH online economic dispatch optimization model considering the uncertainty of wind power.

Meanwhile, the highly efficient and flexible operation of an IES has to be achieved with the support of smart control and communication. Focusing on the coordination optimization of EV charging supplied by DGs in an EI, [42] introduced a simulation-based policy iteration method for event-based optimization based on the performance potentials or Q-factors. The case study proved that the proposed method could alleviate the curses of dimensionality in the Markov decision process, and it could effectively solve the performance optimization problem in discrete event dynamic systems, such as an EI, which is a complex large-scale dynamic system. Reference [43] combined the accurate state information with the inverse process of the system measurement to enhance the accuracy of the resampling process, which was a type of improved

particle filter method used in a stochastic dynamic system of near-surface wind farms. In [44], a cyclic nonhomogeneous Markov chain (CNHMC) steady-state analysis method was designed to represent the variation in the wind power and load during a day. Reference [45] modeled the interaction between the aggregator and two settlement markets as a multistage decision problem, which utilized the information in each intermediate stage between the day-ahead market and the real-time market.

From the above literature, it can be found that the IES has a number of benefits, mainly including developing synergies and complementary advantages of multi–energy for system operation [46], increasing the flexibility and efficiency of systems[47] [48], improving the economic performance[49], and enhancing the system reliability and resilience [50]. However, there are two points that still have not been well addressed:

(i) The model of an integrated energy network structure has been built in several papers. However, how to provide a detailed model for an integrated energy system considering all the network constraints is a crucial issue for further development and efficient operation of the IES.

(ii) Under the multi-energy market, the integrated demand response (IDR) will play a large role in breaking the barriers among the different forms of energy and encouraging the interaction between the supply and demand sides. How to implement the IDR in multi-energy markets is worth studying in detail.

The main contributions of this paper can be summarized as follows:

(i) A tri-layer multi-energy market structure is constructed in which the optimal transaction strategy of the LSE based on the IDR for the purpose of maximum profits is investigated.

(ii) The security operation constraints of the power distribution network, natural gas network and district heating network are explicated modeled in the optimization model.

(iii) To address the uncertainties from the market prices, the conditional value at risk (CVAR) is employed to characterize the risk and a novel CVaR-mean CVaR approach is proposed to mitigate the risk.

The rest of the paper is organized as follows: Section II introduces the modeling of the multi-energy market and optimal transaction strategy of the LSE with consideration of the electricity, heat and natural gas network constraints. Section III considers the uncertainty of forecasted prices with a CVaR-mean CVaR approach. Section IV presents the simulation results of the proposed model on an IEEE 33-bus-11-node-6-node test system. Finally, conclusions are drawn in Section V.

2. Modeling of a Multi-Energy Market

Currently, the electricity market, natural gas market and heat energy market are operating separately. The market mechanisms of the latter two are imperfect, and the prices of natural gas and heat are commonly fixed, which makes it difficult to satisfy the requirements of the optimal allocation of energy market sources and the greatest social benefits. With these considerations, a multi-energy market should be built in which different forms of energy sources are involved and cooperated. Unlike the traditional electricity market, **the multi-energy market allows electricity, natural gas and heat transactions to be developed jointly**. The tri-layer multi-energy market framework is shown in Fig. 1.
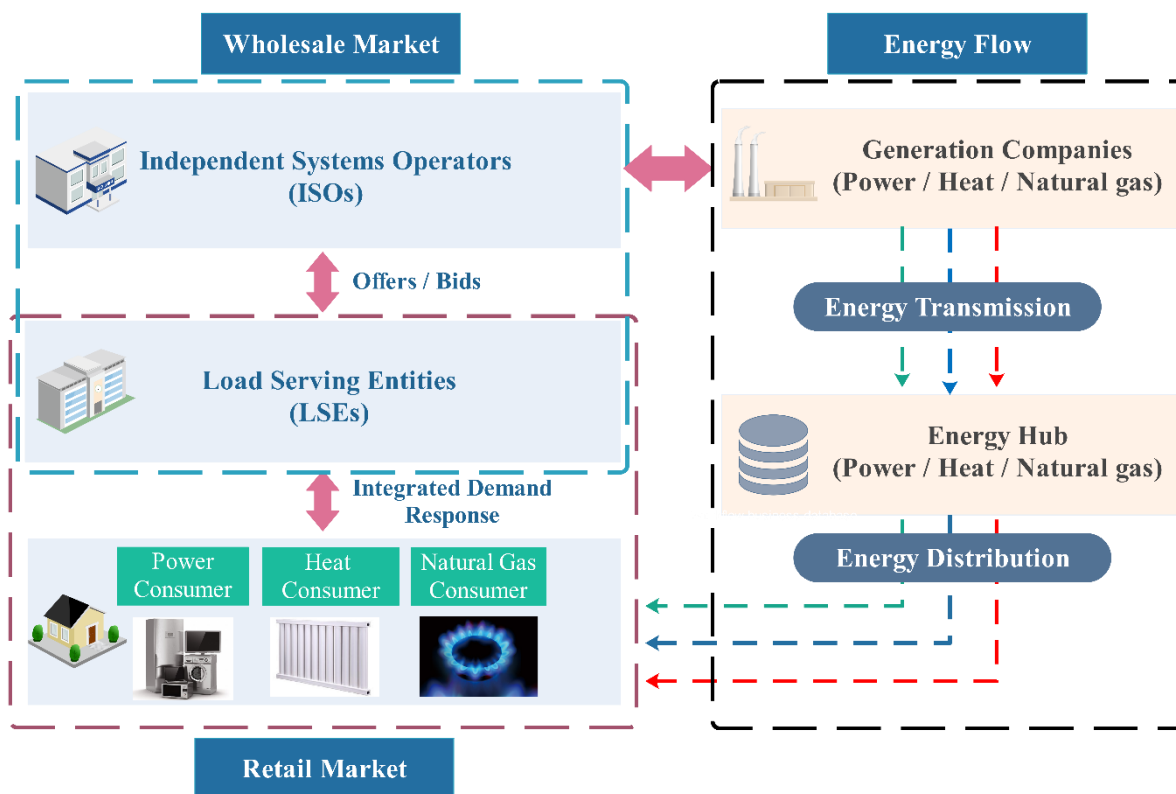
Fig. 1 Tri-layer multi-energy market

The multi-energy market contains multiple energy generators, independent systems operators (ISOs), LSEs and end consumers that use different kinds of energy to meet their demand requirements both in production and life. An ISO receives bid quantity offers from energy generators and LSEs, and then it will subsequently announce clear results in the day-ahead wholesale market. The LSE plays the role of an intermediate bridge between the ISOs and end-users. In particular, the LSE can forecast the energy prices in both the wholesale market and the retail market according to historical data. The end-users' demand data can be received by the LSE through smart energy management systems. Then, the LSE can determine the trading strategy with the ISO based on the predictive market prices and demand data. In this multi-energy market, the LSE is able to buy electricity, gas and heat from the wholesale market to serve retail customers who have barriers in receiving signals of market prices in time. In other words, the LSE prevents its consumers from taking the risk of wholesale market price fluctuations and meets the multi-energy end-users' demand. In this regard, it is important for the LSE to plan the energy trading strategy in each of the 24-hour periods of the day-ahead market.

From the abovementioned market operational mechanism, it can be seen that the LSE is the typical profit seeker in this multi-energy market. To maximize its profit and maintain the satisfaction of its consumers, it is of great significance for the LSE to implement an **integrated demand response (IDR)**. The LSE has three kinds of loads, i.e., electricity loads, natural gas loads and heat loads. Then, the energy types, amount and transaction time are the key issues for the LSE. Generally, the peak and valley hours of electricity price are affected by power user habits. Similarly, price fluctuations exist in both the natural gas prices and heat prices every day. **For the purposes of profit maximization, buying at a low price and selling at a high price is the basic principle and the best choice for the LSE. Based on the curve of the load demand, the LSE can thus determine the energy types and volumes to be purchased and sold via responding to the respective energy market price signals.** For example, in the wholesale market, when the electricity price is higher while the gas price is lower, the LSE will choose to buy more natural gas and less electricity according to the IDR

program. On the other hand, in the retail market, it is a better choice for the LSE to sell more electricity and less natural gas or heat under the same price situation. In other words, the LSE implements an IDR in a multi-energy market by taking advantage of the price variation at different peak and valley periods among electricity, natural gas and heat.

Moreover, the security operation of a multi-energy network should be considered in this model. As Fig. 1 shows, in the energy flow, energy purchased by the LSE will be delivered to the demand side through networks. It is impossible for the LSE to carry on energy transactions ignoring the transmission capacity of networks. Furthermore, to alleviate the contradiction between the LSE's risks arising from market price fluctuation and user satisfaction, an energy hub is necessary for the LSE in a multi-energy market, which will be discussed in detail in section 2.3. Therefore, the model in this paper mainly focuses on an optimal strategy for multi-energy market transactions for the LSE during one day with the explicit consideration of integrated energy network topologies.

2.1 Objective Function

As the interconnection of utilities and end-users in a multi-energy market, an LSE is able to purchase electricity, natural gas and heat from the generation companies with respect to the requirement of different types of energy consumers. In a multi-energy market, the LSE is allowed to buy three kinds of energy simultaneously to maximize the profit, according to the market prices and trading volumes. The profit is the total revenue from consumers minus the cost of buying energy, which are presented in (1), (2) and (3), respectively, as follows:

$$\max \quad Profit = \max \quad \sum_{t=1}^{T}\left(Revenue_t - Cost_t\right) \tag{1}$$

where

$$Cost_t = \rho_{Ps,t}P_{s,t} + \rho_{Gs,t}G_{s,t} + \rho_{Hs,t}H_{s,t}, \quad \forall t \in T \tag{2}$$

$$Revenue_t = \rho_{Pl,t}P_{l,t} + \rho_{Gl,t}G_{l,t} + \rho_{Hl,t}H_{l,t}, \quad \forall t \in T \tag{3}$$

2.2 IDR in the Multi-Energy Market Model

The value of energy purchases at each time period should be limited by the upper and lower bounds as:

$$P_{s,\min} \le P_{s,t} \le P_{s,\max}, \quad \forall s \in \Omega_P^s, t \in T \tag{4}$$

$$G_{s,\min} \le G_{s,t} \le G_{s,\max}, \quad \forall s \in \Omega_G^s, t \in T \tag{5}$$

$$H_{s,\min} \le H_{s,t} \le H_{s,\max}, \quad \forall s \in \Omega_H^s, t \in T \tag{6}$$

An LSE, gathering the load demand data through smart energy meters and energy management systems from end-users, should resell three energy sources to consumers to satisfy their requirements. In equations (7)-(9), the lower bound is determined by the basic load demand that cannot be curtailed while the upper bound is determined by the normal load demand situation. The gap between the upper and lower bound for each load

is elastic and can be adjusted to the price signals, called the demand response. In addition, equation (10) guarantees the minimum energy consumption required by consumers for one day.

$$P_{l,\min} \leq P_{l,t} \leq P_{l,\max}, \quad \forall l \in \Omega_P^{load}, t \in T \tag{7}$$

$$G_{l,\min} \leq G_{l,t} \leq G_{l,\max}, \quad \forall l \in \Omega_G^{load}, t \in T \tag{8}$$

$$H_{l,\min} \leq H_{l,t} \leq H_{l,\max}, \quad \forall l \in \Omega_H^{load}, t \in T \tag{9}$$

$$P_{l,day} \leq \sum_{t=1}^{T} P_{l,t} \quad \forall l \in \Omega_P^{load} \qquad G_{l,day} \leq \sum_{t=1}^{T} G_{l,t} \quad \forall l \in \Omega_G^{load} \qquad H_{l,day} \leq \sum_{t=1}^{T} H_{l,t} \quad \forall l \in \Omega_H^{load} \tag{10}$$

To meet the reliability requirement for the three types of energies, a certain value of reservation has to be purchased to guarantee sufficient energy for the end-users. Thus, the total energy for one day should be greater than the total value of load demand plus the value of reserve, giving the following:

$$\sum_{t=1}^{T} P_{s,t} \geq RES_P + \sum_{t=1}^{T} P_{l,t}, \quad \forall s \in \Omega_P^s, l \in \Omega_P^{load} \tag{11}$$

$$\sum_{t=1}^{T} G_{s,t} \geq RES_G + \sum_{t=1}^{T} G_{l,t}, \quad \forall s \in \Omega_G^s, l \in \Omega_G^{load} \tag{12}$$

$$\sum_{t=1}^{T} H_{s,t} \geq RES_H + \sum_{t=1}^{T} H_{l,t}, \quad \forall s \in \Omega_H^s, l \in \Omega_H^{load} \tag{13}$$

2.3 Multi-energy Coupling Model

In a multi-energy market, an energy hub (EH) can implement the energy transformation, distribution and storage among different types of energies. As shown in Fig. 2, an EH is composed of multi-energy inputs, conversions and outputs. Three types of energy flows, including electricity, natural gas and heat, are injected into energy hubs. They can be converted by different devices, such as gas-fired combined heat and power (CHP), heat pumps, electric boilers, power to gas equipment (P2G), combined cycle gas turbines (CCGT), etc. Furthermore, the energy storage device in the EH can achieve peak shifting for each type of energy by charging/discharging at any trading period. The energy redistribution and storage of an EH make it more flexible and active for the LSE with the consideration of the IDR.
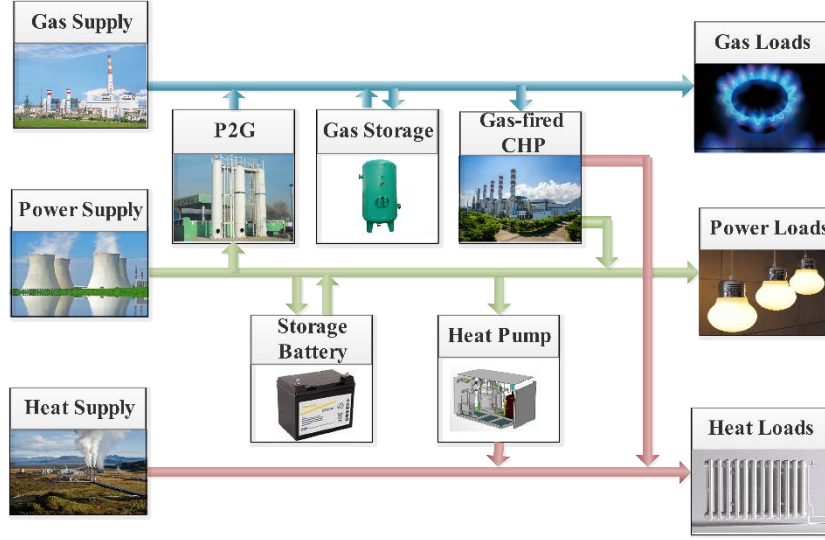
Fig. 2 Multi-energy coupling model

Then, the mathematical model of the EH unit is introduced in Fig. 3. The conversion relationship between the single input energy α and single output energy β can be expressed as follows:

$$E_\beta = \gamma_{\alpha\beta} E_\alpha \tag{14}$$

The coefficient $\gamma_{\alpha\beta}$ varies with the input energy, which can be represented as the function of input energy, such that:

$$\gamma_{\alpha\beta} = f_\beta(E_\alpha) \tag{15}$$

For the sake of simplicity, the coupling coefficient $\gamma_{\alpha\beta}$ is regarded as a constant value that is derived from energy conversion efficiencies. Ref. **Error! Reference source not found.** has indicated that the constant coupling coefficient has no influence on the accuracy of the model. In an EH, the electricity, natural gas and heat can be transmitted and converted. In particular, the input energy can be delivered to the output directly through transmission networks, such as overhead lines or pipelines, or transformed into another form by converters mentioned above. Therefore, the energy balance between the input and output can be given as follows:

$$\begin{bmatrix} P_{out,t} \\ G_{out,t} \\ H_{out,t} \end{bmatrix} = A \times \begin{bmatrix} P_{in,t} \\ G_{in,t} \\ H_{in,t} \end{bmatrix}, \quad \forall t \in T \tag{16}$$

$$A = \begin{bmatrix} \gamma_P & \gamma_{GP} & \gamma_{PH} \\ \gamma_{GP} & \gamma_G & \gamma_{GH} \\ \gamma_{HP} & \gamma_{HG} & \gamma_H \end{bmatrix} \tag{17}$$

The main diagonal elements in A represent the transmission efficiency of electricity, heat and natural gas, respectively. The nondiagonal elements in matrix A represent the conversion efficiency between the input

energy and output energy. Because there is no device for converting the heat into electricity in actual production, γ_{HP} and γ_{HG} are set to zero.
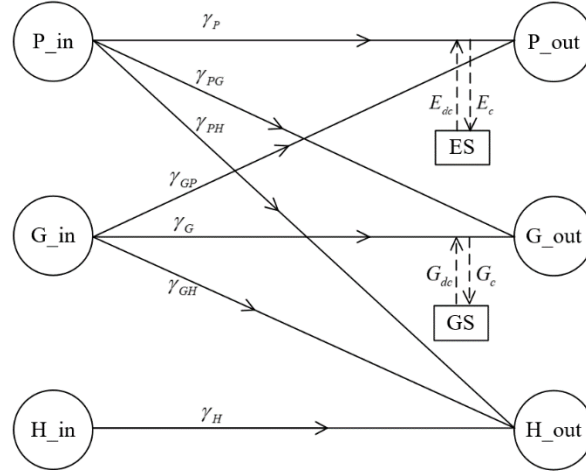

Fig. 3 Mathematical model of an energy hub

Because the LSE can dispatch the charging and discharging of energy storage during trading periods, the energy balance of an EH should take energy storage into consideration. Thus, according to Fig. 3, equation (16) can be substituted by (18) as follows:

$$\begin{bmatrix} P_{out,t} \\ G_{out,t} \\ H_{out,t} \end{bmatrix} = A \times \begin{bmatrix} P_{in,t} \\ G_{in,t} \\ H_{in,t} \end{bmatrix} + \begin{bmatrix} P_{dc,t} \\ G_{dc,t} \\ 0 \end{bmatrix} - \begin{bmatrix} P_{c,t} \\ G_{c,t} \\ 0 \end{bmatrix}, \quad \forall t \in T \tag{18}$$

It should be noted that energy storage devices in this model includes storage battery and gas tanks. Unlike power energy, natural gas can be stored on a large scale, so a gas storage tank is usually installed on the natural gas demand side to enhance the flexibility and reliability of the natural gas system operation. Natural gas can be injected into storage facilities during low load periods and can be withdrawn from storage facilities during peak load periods. In actual operation, the total gas volume reserved in storage at a particular moment t is related to the amount of stored gas at period t-1 and the injection-deliverable state at period t as follows:

$$GS_t = GS_{t-1} + G_{c,t}\zeta_G - G_{dc,t} / \zeta_G, \quad \forall t \in T \tag{19}$$

Meanwhile, the sum of injection during the entire trading period T should be equal to the sum of output:

$$\sum_{t=1}^{T} G_{c,t} = \sum_{t=1}^{T} G_{dc,t} \tag{20}$$

The total gas reserved in storage and the injection-deliverable state are subject to the following constraints:

$$GS_{\min} \leq GS_t \leq GS_{\min}, \quad \forall t \in T \tag{21}$$

$$G_{c,\min} \leq G_{c,t} \leq G_{c,\min}, \quad \forall t \in T \tag{22}$$

$$G_{dc,\min} \leq G_{dc,t} \leq G_{dc,\min}, \quad \forall t \in T \tag{23}$$

The storage characteristics of storage battery in power system, are similar to those of a gas tank, which are given in the appendix (A1)-(A5).

2.4 Power Distribution Network Constraints

A power distribution network branch flow model based on second-order cones can solve the optimal power flow efficiently by two relaxation steps: the first step eliminates the voltage and current angles, and the second step approximates the resulting problem by conic programming.
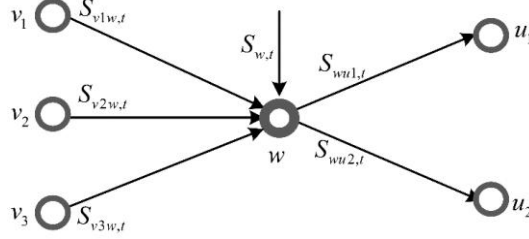

Fig. 4 Radial network schematic

Fig. 4 depicts the typical model of a radial network. The branch flow model mainly focuses on the currents and powers of the branches in the radial network. The basic branch flow model is given in (24)-(26), including the power balance at each bus, Ohm's law on each branch and complex power at the beginning of each branch.

$$S_{w,t} = \sum_{(w,u)\in\Omega_P^{branch}} S_{wu,t} + \sum_{(v,w)\in\Omega_P^{branch}} (-S_{vw,t} + z_{vw}|I_{vw,t}|^2), \quad \forall w \in \Omega_P^{bus}, t \in T \tag{24}$$

$$V_{w,t} - V_{u,t} = z_{wu}I_{wu,t}, \quad \forall w,u \in \Omega_P^{bus}, t \in T \tag{25}$$

$$S_{wu,t} = V_{w,t}I_{wu,t}^*, \quad \forall w,u \in \Omega_P^{bus}, t \in T \tag{26}$$

where (w, u) indicates that the branch is from bus w to bus u.

Furthermore, equation (24) can be expressed as the real variables given in (27) and (28). Substituting (25) into (26) and squaring both sides equation (29) is obtained.

$$P_{w,t} = \sum_{(w,u)\in\Omega_P^{branch}} P_{wu,t} + \sum_{(v,w)\in\Omega_P^{branch}} (-P_{vw,t} + r_{vw}|I_{vw,t}|^2), \quad \forall w,u,v \in \Omega_P^{bus}, t \in T \tag{27}$$

$$Q_{w,t} = \sum_{(w,u)\in\Omega_P^{branch}} Q_{wu,t} + \sum_{(v,w)\in\Omega_P^{branch}} (-Q_{vw,t} + x_{vw}|I_{vw,t}|^2), \quad \forall w,u,v \in \Omega_P^{bus}, t \in T \tag{28}$$

$$\upsilon_{w,t}^2 - \upsilon_{z,t}^2 = 2(r_{wz}P_{wz,t} + x_{wz}Q_{wz,t}) - (r_{wz}^2 + x_{wz}^2)|I_{wz,t}|^2, \quad \forall (w,z) \in \Omega_P^{branch}, t \in T \tag{29}$$

$$P_{wz,t}^2 + Q_{wz,t}^2 = \upsilon_{w,t}|I_{wz,t}|^2, \quad \forall (w,z) \in \Omega_P^{branch}, t \in T \tag{30}$$

Since the quadratic constraint (30) leads to the nonconvex feasible region of the optimization model, this paper employs a second-order cone relaxation technique to relax the nonconvex feasible region, giving the following:

$$P_{wz,t}^2 + Q_{wz,t}^2 \le \upsilon_{w,t} \left| I_{wz,t} \right|^2, \quad \forall (w,z) \in \Omega_P^{branch}, t \in T \tag{31}$$

The current magnitude on each branch and the voltage magnitude on each node should be restricted within the corresponding lower and upper bounds as follows:

$$I_{wz,\min} \le I_{wz,t} \le I_{wz}, \quad \forall wz \in \Omega_P^{branch}, t \in T \tag{32}$$

$$\upsilon_{w,\min} \le \upsilon_{w,t} \le \upsilon_{w,\max}, \quad \forall w \in \Omega_P^{bus}, t \in T \tag{33}$$

2.5 Natural Gas Network Constraints

A typical gas distribution network consists of gas suppliers, compressors, natural gas pipelines and gas loads. Natural gas can be transported to gas loads by rail or sea using liquefied natural gas tanks as well as natural gas pipelines. As natural gas pipelines can transport natural gas across a long distance and on a large scale, pipeline transport has become one of the main means of natural gas transmission. Generally, the pressure of the natural gas pipeline will gradually decline due to the friction between the natural gas flow and the pipeline wall. Therefore, it is often necessary to install a compressor to ensure the pressure within the normal working range when delivering natural gas over long distances. The function of the compressor in a natural gas network is similar to a transformer in a power system. The structure of the natural gas network is shown in Fig. 5.

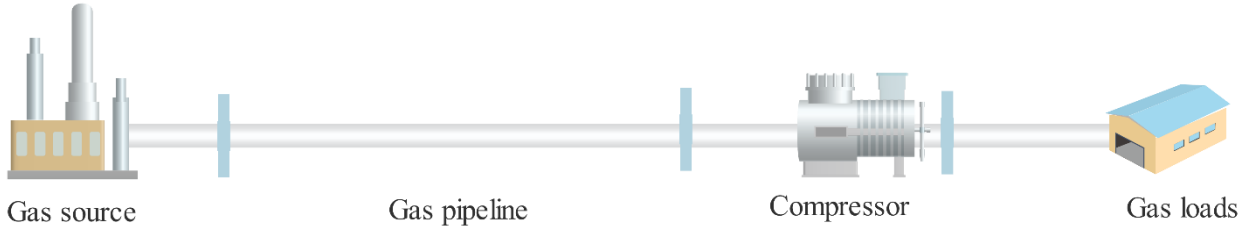Gas source   Gas pipeline   Compressor   Gas loads

Fig. 5 Natural gas network

Limited by the physical characteristics of pipelines such as friction, length and diameter, the gas flow in a pipeline and the nodal pressures are given by:

$$fp_{p,\min} \le fp_{p,t} \le fp_{p,\max}, \quad \forall p \in \Omega_G^{pipe}, t \in T \tag{34}$$

$$\pi_{n,\min} \le \pi_{n,t} \le \pi_{n,\max}, \quad \forall n \in \Omega_G^{node}, t \in T \tag{35}$$

The transportation of natural gas in the network depends on the pressure difference at both ends of the natural gas pipeline. The Weymouth gas flow equation is used in this model.

$$sgn(fp_{p,t}) fp_{p,t}^2 = \phi_{p,t}(\pi_{i,t}^2 - \pi_{j,t}^2), \quad \forall p \in \Omega_G^{pipe}, t \in T \tag{36}$$

$$sgn(fp_{p,t}) = \begin{cases} +1 & \pi_{i,t} > \pi_{j,t} \\ -1 & \pi_{i,t} < \pi_{j,t} \end{cases} \tag{37}$$

The gas flows are delivered from high pressure nodes to low pressure nodes. Noting that gas flow is positive if the starting node i of the gas pipeline p is higher than its ending node j, vice versa.

13

Obviously, the Weymouth gas flow equation expressed in (36) is nonconvex and nonlinear, which increases the complexity of the natural gas network model. To simplify the model, replacing the squared node pressure by *ps* eliminates the nonlinearity, such that:

$$ps_{i,t} = \pi_{i,t}^2 \ , \quad \forall p \in \Omega_G^{pipe}, t \in T \tag{38}$$

Then, equation (36) can be expressed as follows:

$$sgn(fp_{p,t})fp_{p,t}^2 = \phi_{p,t}(ps_{i,t} - ps_{j,t}), \quad \forall p \in \Omega_G^{pipe}, t \in T \tag{39}$$

Unfortunately, the left-hand side of equation (40) is still nonlinear. Furthermore, the piecewise linearization technique will be used to linearize the nonlinear term $sgn(fp_p)fp_p^2$, as follows:

(1) The proper number of linear segments should be set considering the trade-off between the approximation accuracy and computational complexity.

(2) The continuous variable *fp* can be divided into a series of discrete segment points LFP_k according to the number of linear segments.

(3) The value of the function corresponding to each discrete point is LFP_k^2.

(4) Then, *fp* and $sgn(fp_p)fp_p^2$ are linearized by introducing new continuous variables δ and binary variables η through a piecewise linearization program in equations (40)-(43).

Assuming that LFP_k represents a series of discrete segment points of the continuous variable *fp*, new variables δ are introduced. Thus, the piecewise linearized equation is given in equation (40), and the discrete variables of gas flow are represented by equation (41). Constraints (42) and (43) ensure the continuity of sections.

$$LFP_{p,1,t}^2 + \sum_{k=1}^{NPL-1} (LFP_{p,k+1,t}^2 - LFP_{p,k,t}^2)\delta_{p,k,t} = \phi_p(ps_{i,t} - ps_{j,t}), \quad \forall p \in \Omega_G^{pipe}, t \in T \tag{40}$$

$$LFP_{p,t} = LFP_{p,1,t} + \sum_{k=1}^{NPL-1} (LFP_{p,k+1,t} - LFP_{p,k,t})\delta_{p,k,t}, \quad \forall p \in \Omega_G^{pipe}, t \in T \tag{41}$$

$$\delta_{p,k+1,t} \leq \eta_{p,k,t}, \eta_{p,k,t} \leq \delta_{p,k,t}, \quad \forall p \in \Omega_G^{pipe}, t \in T, k = 1,2,...,NPL-2 \tag{42}$$

$$0 \leq \delta_{p,k,t} \leq 1, \eta_{p,k,t} \in \{0,1\}, \quad \forall p \in \Omega_{G,}^{pipe}, t \in T, k = 1,2,...,NPL-1 \tag{43}$$

Due to the pressure loss in the gas transmission network, several compressors should be installed to compensate for the pressure loss and ensure the transmission reliability. For simplicity, the energy consumption of the compressor is ignored, while the inlet and outlet pressures are considered in this paper, which can be modeled as follows:

$$\pi_{cm,t} \leq \pi_{cn,t} \leq \gamma_0 \pi_{cm,t}, \quad \forall t \in T \tag{44}$$

During the operation of the gas network, the gas flow balance at any node should be ensured. An equation for the mass continuity at each node is given as follows:

$$\sum_{k\in\Omega_G^{pipe}} B_{nk} fp_{k,t} + \sum_{s\in\Omega_G^s} C_{ns} G_{s,t} - \sum_{l\in\Omega_G^{load}} D_{nl} G_{l,t} = 0, \quad \forall n \in \Omega_G^{node} \; t \in T \tag{45}$$

2.6 District Heating Network Constraints

The district heating system (DHS) consists of three parts: the heat sources, heating network, and heat load. The typical DHS structure is shown in Fig. 6. The heat sources in a DHS are the heating equipment for the heat transmission medium (steam or hot water) by using the thermal energy generated by fuel combustion. Generally, combined heat and power (CHP), heat pumps, and electric boilers are the typical heat sources in a DHS. The heating network is a water circular system, including a supply network and return network with similar network topology. Practically, the supply pipes transfer hot water from a central heat source to the residential, commercial and industrial heat loads. After cooling, the cold water enters the return pipe to be recycled. A heat exchanger is used for concentrating and exchanging the heat in the network, similar to the functionality of a transformer in a power grid. The heat loads mainly include domestic hot water supply systems, production hot water systems and heating equipment.
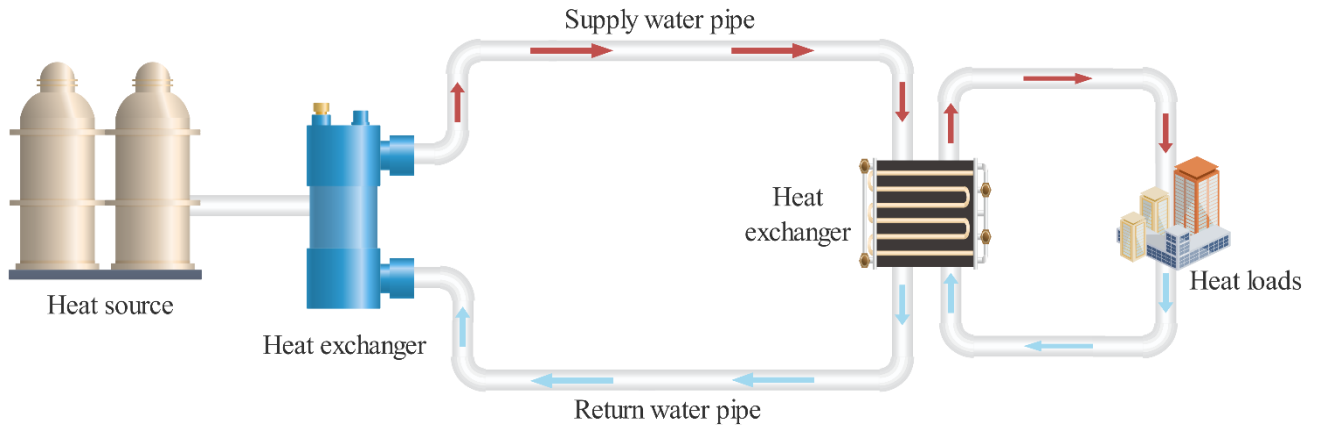

Fig. 6 District heating system

From the perspective of DHS operation, the supply temperature and mass flow rate are the two key elements controlling the operating mode of the DHS. There are four types of operating strategies for a DHS to satisfy the requirements of the heat consumers, i.e., CF-CT, CF-VT, VF-CT and VF-VT [51]. Considering the accuracy and maintaining the simplicity of the model at the same time, a constant flow and variable temperature (CF-VT) operating control strategy is used in this DHS model. This means that the flow rate can be assumed to be a constant, while the supply temperature is regarded as a variable according to the heat loads during daily operation.

(1) Heat sources

The heat output of the heat source is determined by the temperature difference between the supply network and the return network, which can be given by:

$$H_{s,t} = c m_{j,t}^{HS} (\tau_{n,t}^S - \tau_{n,t}^R), \quad \forall s \in \Omega_H^s, \; j \in \Omega_{HS}^{pipe}, n \in \Omega_{HS}^{node}, t \in T \tag{46}$$

The supply temperature of the heat source should be limited by the lower and upper bounds as

$$\tau_{n,\min}^{S} \leq \tau_{n,t}^{S} \leq \tau_{n,\max}^{S}, \quad \forall n \in \Omega_{HS}^{node}, t \in T \tag{47}$$

(2) Heat exchangers

A heat network can be regarded as a combination of the transmission and distribution network. Heat exchangers play important roles in the energy exchange between the hot water in the supply pipeline and the cold water in the return pipeline. Therefore, they are usually installed between the heat sources and transmission networks or between the distribution network and each customer. Thus, the heat exchangers can be regarded as the heat loads from the demand side.

$$H_{l,t} = c\, m_{l,t}(\tau_{n,t}^{S} - \tau_{n,t}^{R}), \quad \forall l \in \Omega_{HL}^{pipe}, n \in \Omega_{HL}^{node}, t \in T \tag{48}$$

$$\tau_{n,\min}^{R} \leq \tau_{n,t}^{R} \leq \tau_{n,\max}^{R}, \quad \forall n \in \Omega_{HL}^{node}, t \in T \tag{49}$$

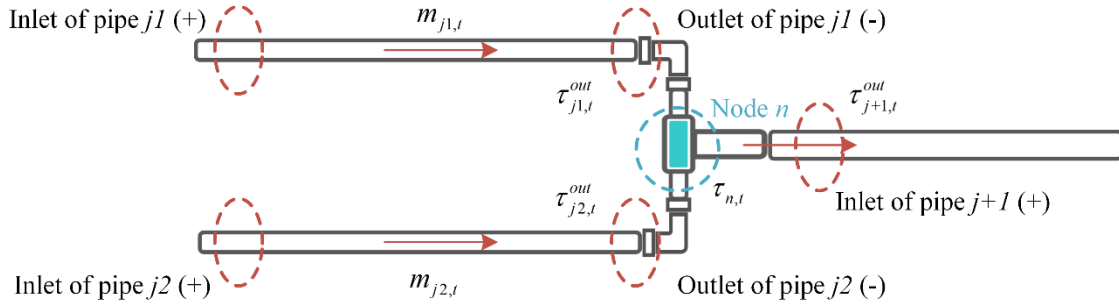### (3) District heating network

Fig. 7 General structure of nodes and pipelines in DHS

As mentioned above, the mass flow rate in the heating network is fixed because the CF-VT control strategy is used in the DHS. To clarify, Fig. 7 describes a general structure of the nodes and pipelines in the DHS. Due to the same topology of the supply network and return network, Fig. 7 only expresses the one-way pipes of the DHS, which is applicable to both the supply water pipes and return water pipes. The injected mass flow from multiple pipes is mixed at the same node, then the relationship between the mixed temperature at each node and the outlet temperature of the connected pipeline can be given as follows:

$$\sum_{j \in \Omega^{Spipe^{-}}} (\tau_{j,t}^{S}, m_{j,t}^{S}) = \tau_{n,t}^{S} \sum_{j \in \Omega^{Spipe^{-}}} m_{j,t}^{S}, \quad \forall n \in \Omega_{H}^{node}, t \in T \tag{50}$$

$$\sum_{j \in \Omega^{Rpipe^{-}}} (\tau_{j,t}^{R}, m_{j,t}^{R}) = \tau_{n,t}^{R} \sum_{j \in \Omega^{Rpipe^{-}}} m_{j,t}^{R}, \quad \forall n \in \Omega_{H}^{node}, t \in T \tag{51}$$

The temperature at the inlet of each pipeline, namely, the temperature of mass flowing out of the pipe, is equal to the mixed temperature of its start node.

$$\tau_{j,t}^{S} = \tau_{n,t}^{S} \quad \forall j \in \Omega^{Spipe^{+}}, \quad \forall n \in \Omega_{H}^{node}, t \in T \tag{52}$$

$$\tau_{j,t}^{R} = \tau_{n,t}^{R} \quad \forall j \in \Omega^{Rpipe^{+}}, \quad \forall n \in \Omega_{H}^{node}, t \in T \tag{53}$$

There is heat loss at each pipeline due to the roughness of the pipe and surrounding temperature, which results in a temperature drop between the inlet and outlet. A linearization of the temperature drop model can be used to express their relationship.

$$\tau_{j,t}^{S,out} = (\tau_{j,t}^{S,in} - \tau_g)(1 - \frac{U_j l_j}{c\, m_{j,t}^S}) + \tau_g, \quad \forall j \in \Omega_H^{Spipe}, t \in T \tag{54}$$

$$\tau_{j,t}^{R,out} = (\tau_{j,t}^{R,in} - \tau_g)(1 - \frac{U_j l_j}{c\, m_{j,t}^R}) + \tau_g, \quad \forall j \in \Omega_H^{Rpipe}, t \in T \tag{55}$$

The heat loss in each pipeline is determined by the inlet and outlet temperatures.

$$H_{loss,j,t} = c\, m_{j,t}(\tau_{j,t}^{in} - \tau_{j,t}^{out}), \quad \forall j \in \Omega^{pipe}, n \in \Omega_H^{node}, t \in T \tag{56}$$

3. A CVaR-mean CVaR Approach for Uncertain Prices

It can be observed that the previous model is mathematically a mixed integer second order cone programming process, which is conducted under deterministic parameters (i.e., the prices are given as the forecasted values). The compact formulation can be written as follows:

$$\max_x \quad F(x, \rho), \quad x \in \Omega \tag{57}$$

where x is the vector of decision variables, ρ is the uncertain parameters (i.e., the prices), F(x, ρ) is the profit function, and Ω is the feasible region of the decision variables.

However, the forecasted prices are generally uncertain which will bring risk to the profit of the decision makers. To address this problem, the CVaR can be used to measure the risk resulting from the uncertain prices. The CVaR, derived from the loss distribution, involves discreetness which will be better than the value at risk (VaR). Since the VaR and CVaR are used for the loss function, the loss function $f(x, \rho)$ of the profit function $F(x, \rho)$ satisfies that $f(x,\rho) = -F(x,\rho) = -\rho^T x$. As a result, for a given confidence level α, the general expression of the VaR is given as follows:

$$VaR_\alpha(x) = \min\left\{\gamma | \int_{f(x,\rho) \le \gamma} p(\rho) d\rho \ge \alpha\right\} \tag{58}$$

where $p(\rho)$ is the probability distribution function of the uncertain prices. Based on the definition of VaR, the CVaR associated with the decision variables x can be written as follows:

$$CVaR_\alpha(x) = \frac{1}{1-\alpha} \int_{f(x,\rho) \ge VaR_\alpha(x)} f(x, \rho) p(\rho) d\rho \tag{59}$$

As proved in [53], CVaR is not always smaller than the VaR for any confidence level α and has more advantages than the VaR. Furthermore, to facilitate the computation in the optimization problem, an auxiliary function is introduced as:

$$G_\alpha(x, \gamma) = \gamma + \frac{1}{1-\alpha} \int (f(x, \rho) - \gamma)^+ p(\rho) d\rho \tag{60}$$

17

With the consideration of N_v independent samples for the probability distribution $p(\rho)$, denoted as (ρ_1, ρ_2, …, ρ_{N_v}), (60) can be approximated as (61) by substituting $f(x,\rho) = -\rho^T x$ into (60).

$$\overline{G}_\alpha(x,\gamma) = \gamma + \frac{1}{N_v(1-\alpha)}\sum_{v=1}^{N_v}\left(-\rho_v^T x - \gamma\right)^+ \tag{61}$$

For the portfolio optimization of the original model (57), mean-variance analysis can provide a tradeoff between the profit and risk due to the uncertainties. As presented before, the CVaR is a kind of measure to describe the risk. Therefore, a mean CVaR aims to maximize the total profit while minimizing the return risk. For the probability distribution $p(\rho)$, we can easily estimate the mean value of the uncertain price ρ as μ, which leads to the mean CVaR optimization model as follows:

$$\min_{x,\gamma} \quad -\mu^T x + \lambda\left(\gamma + \frac{1}{N_v(1-\alpha)}\sum_{v=1}^{N_v}\left(-\rho_v^T x - \gamma\right)^+\right), \quad s.t. \quad x \in \Omega \tag{62}$$

where λ is the risk preference factor. Moreover, $\left(-\rho_v^T x - \gamma\right)^+ = \max\left(-\rho_v^T x - \gamma, 0\right)$, which can be reformulated by two inequality constraints.

$$\min_{x,\gamma,z} \quad -\mu^T x + \lambda\left(\gamma + \frac{1}{N_v(1-\alpha)}\sum_{v=1}^{N_v}z_v\right), \quad s.t. \quad x \in \Omega, \ z_v \geq -\rho_v^T x - \gamma, \ z_v \geq 0, \ \text{for } v=1, \ …, \ N_v \tag{63}$$

where z_v is a dummy continuous variable that denotes the choice of $-\rho_v^T x - \gamma$ or 0.

Unfortunately, the probability distribution function $p(\rho)$ is still uncertain in the real world. That means, the estimated mean value μ could be subject to estimation errors, which will lead to a large bias of the optimal portfolio against the true value. Because the CVaR is utilized for addressing the risk of uncertainties, the basic idea of the proposed method in this paper is to use the CVaR again to measure the uncertain mean value μ, forming the CVaR-mean CVaR approach. Similar to (61), considering that there are N_μ independent samples for the uncertain mean value of the prices, denoted as (μ_1, μ_2, …, μ_{N_ϑ}), the CVaR-mean CVaR optimization model yields the following:

$$\min_{x,\gamma,z,o,\eta} \quad \eta + \frac{1}{N_\mu(1-\alpha)}\sum_{\vartheta=1}^{N_\mu}o_\vartheta + \lambda\left(\gamma + \frac{1}{N_v(1-\alpha)}\sum_{v=1}^{N_v}z_v\right) \tag{64a}$$

$$s.t. \quad x \in \Omega, \tag{64b}$$

$$z_v \geq -\rho_v^T x - \gamma, \ z_v \geq 0, \ \text{for } v=1, \ …, \ N_v, \tag{64c}$$

$$o_\vartheta \geq -\mu_\vartheta^T x - \eta, \ o_\vartheta \geq 0, \ \text{for } \vartheta=1, \ …, \ N_\vartheta \tag{64d}$$

where o_g is a dummy continuous variable that denotes the choice of $-\mu_g^T x - \eta$ or 0.

4. Case Study

In this section, the LSE's optimal trading strategies in a multi-energy market are verified on an IES consisting of an IEEE 33-bus power distribution network, an 11-node gas network [52] and a 6-node heating network [25]. As shown in Fig. 8, the energy convertors in the EH include a gas-fired CHP, electric boiler and P2G. Node 4 in the natural gas network supplies the fuel for the gas-fired CHP connected to node 1 in the heat system and bus 2 in the power system. The electric boiler combines bus 7 in the power system with node 1 in the heat system. Bus 25 in the power system is connected to node 3 in the gas system through P2G. Moreover, storage battery is installed on bus 17 in the power system while gas storage is on node 7 in gas network. The compression ratio of gas compressor on pipeline 11 is set to 1.2. The parameters in Multiple energy coupling matrix A in the EH is set in (65). All the detailed operation parameters of IES network are available from Table AI-AⅢ in appendix.

$$A = \begin{bmatrix} 0.94 & 0.35 \\ 0.60 & 0.80 \\ 0.90 & 0.80 \end{bmatrix} \tag{65}$$
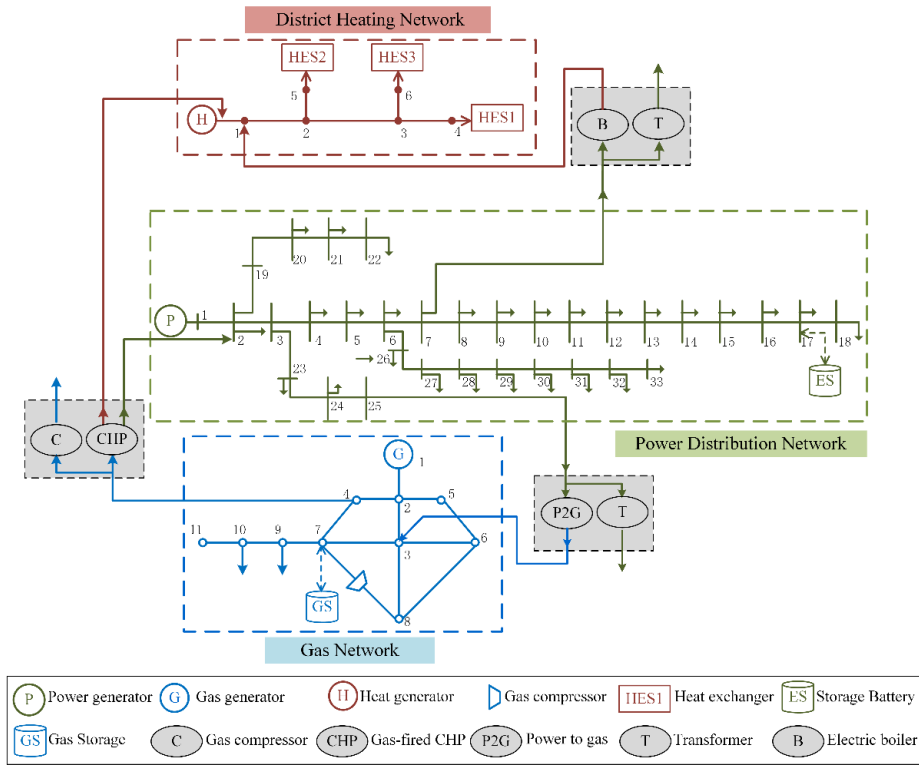

Fig. 8 Integrated energy system

Assuming that the wholesale energy prices and retail energy prices can be forecasted by the LSE, the confidence level of the wholesale market price is chosen as 0.95 to characterize the uncertainties and the risk preference factor λ is chosen to be 0.01. The 24-hour wholesale market real-time prices and TOU prices of electricity, heat and natural gas are shown in Fig. 9. Here, we consider that the different types of energy prices may be at different peak price periods. The electricity price is higher at 8:00-13:00 and 18:00-21:00, the heat price is higher at 22:00-24:00 and 1:00-6:00, while the natural gas price peak is higher at 9:00-17:00. Then, a

series of contrasting cases, including three independent markets, the electricity-gas market, the electricity-heat market and the multi-energy market proposed in this paper, will be discussed in detail as follows.
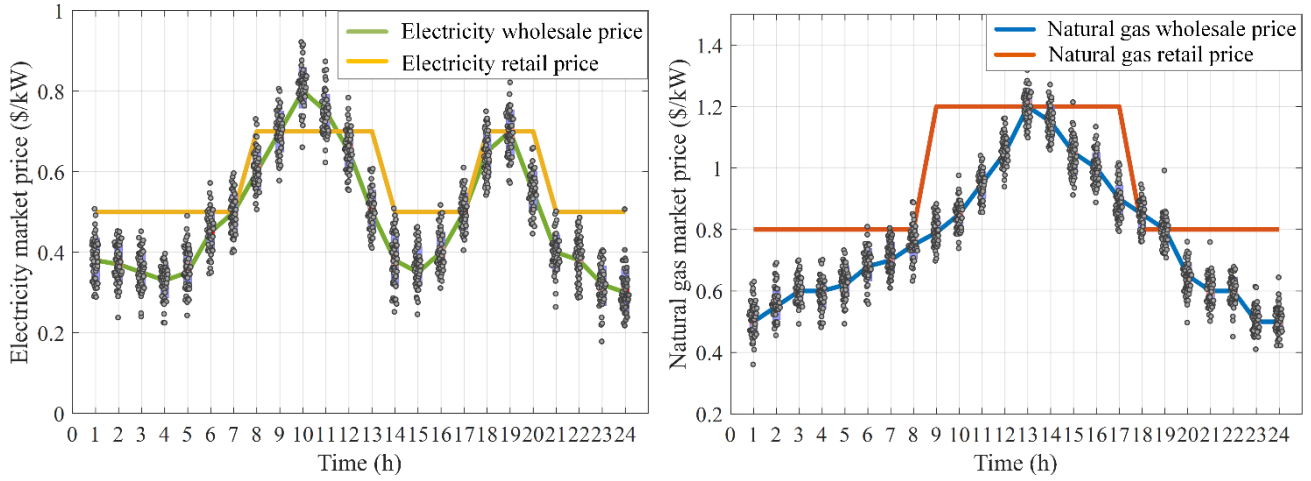
(a) Electricity market price during 24 hours

(b) Natural gas market price during 24 hours
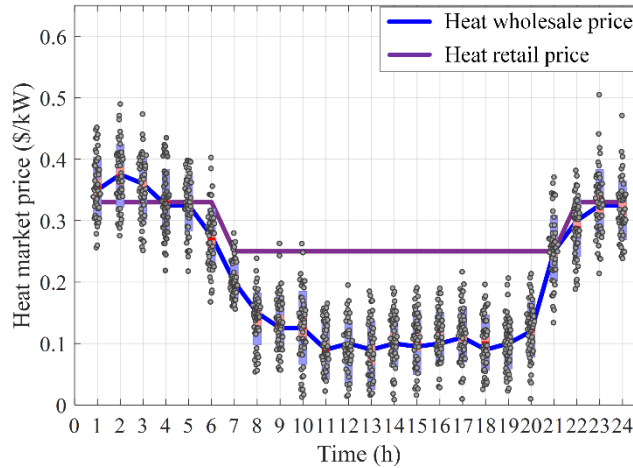
(c) Heat market price during 24 hours

Fig. 9 Energy market prices

4.1 Case A: Three independent energy markets

Case A is carried out in three traditional independent energy markets, which means that the electricity market, heat market and natural gas market operate separately without the connection. The LSE can only implement a traditional DR program in the three corresponding markets.

Fig. 10 shows the energy trading results of the LSE in three independent markets. Note that the energy purchases in the wholesale market are positive, while the energy sales in the retail market are negative. For the purpose of maximum profit, the LSE will choose to buy electricity when its wholesale price is lower, while it sells electricity when the retail price is higher all while guaranteeing the physical constraints. And thanks to storage battery, the LSE can achieve peak shaving via charging at price trough and discharging at price peak time. The same is true in gas market. It can be noticed in Fig. 10(a) that the transaction volume decreases largely at 10:00, this is because the wholesale price is higher than retail price at this period. Obviously, it is unwise for the LSE to purchase too much electricity from market directly. Instead, discharging power from

storage battery to satisfy market demand is a better choice for LSE. The same situation turns out in gas market at 13:00 and in heat market at 1:00-4:00. Unfortunately, since energy storage device is not considered in DHS, LSE can only earn profit by simply buying and selling heat in its market.

Table I summarizes the profit of the LSE in detail, and the total profit of the LSE in the three independent markets is $125.0374. Table II shows the difference between the peak load and valley load. In isolated markets discussed in case A, it is only influenced by market demand and charging-discharging of energy storage. While if multi-energy conversion is considered, the peak-valley differences are affected also by convertors in EH.
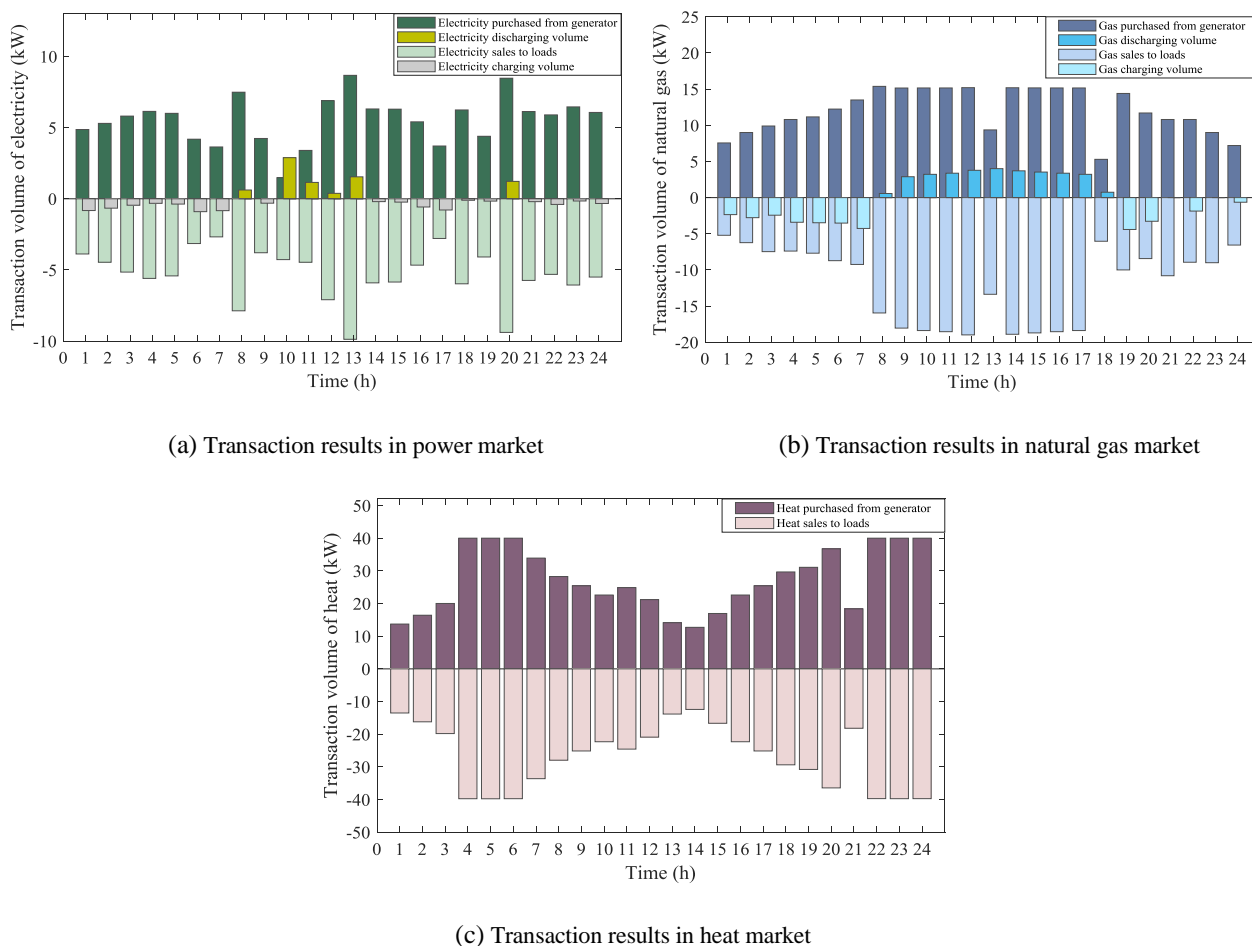

(a) Transaction results in power market

(b) Transaction results in natural gas market

(c) Transaction results in heat market

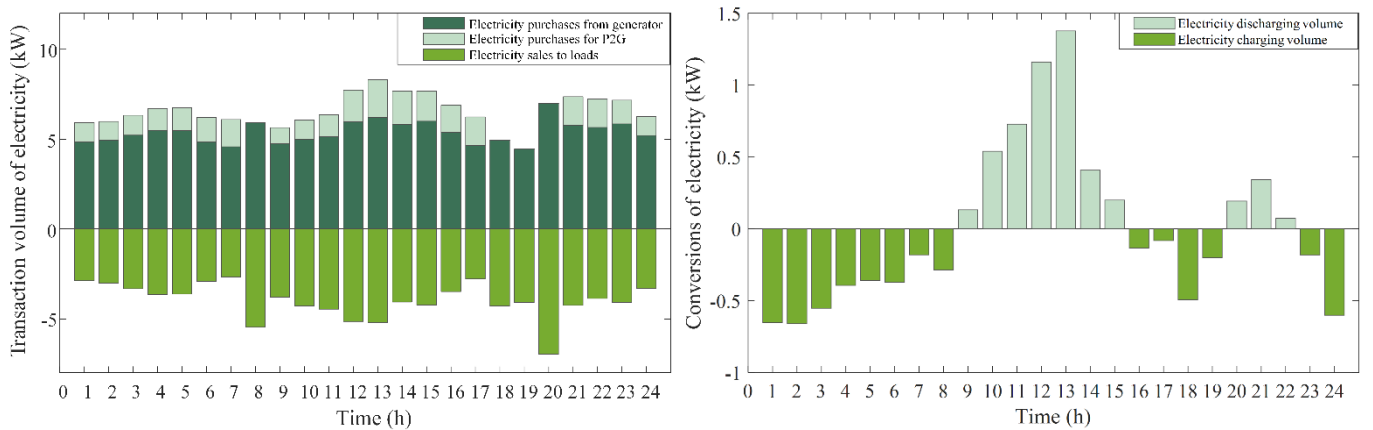Fig. 10. Transaction results of the LSE in three independent markets

Table I Total profits of the LSE in different markets

| Market category	Profit of electricity trades ($)	Profit of gas trades ($)	Profit of heat trades ($)	Gross profit ($)
Electricity market	13.138	\	\	13.138
Natural gas market	\	65.566	\	65.566
Heat market	\	\	46.3334	46.3334
EGM	-18.2493	110.5787	\	92.3294
EHM	7.5832	\	55.4785	63.0617
Multi-energy market (case C)	-20.3976	97.1529	87.4267	164.1821
Multi-energy market (case D)	- 15.5140	96.2025	95.3664	176.0549

4.2 Case B: Electricity-gas market and electricity-heat market

Two contrast tests are given in this case. The histograms on the left in Fig.11 show the optimal electricity-gas purchase and sale volume and trading hours of the LSE in the EGM, while the histogram on the right is the energy conversion of EH in this market, including the effect of storage devices and P2G.

In the electricity-gas market (EGM), based on the electricity demand and gas demand, the LSE is allowed to buy electricity and gas in a 24-hour period according to the respective market prices. P2G is used to convert electricity to natural gas in the EGM. The LSE is responsible for serving its power users and gas users. Usually, the market price is proportional to the load demand, which means the LSE has to purchase a large amount of energy to fulfill the user demand even though the wholesale price is quite high. Obviously, it violates the profit principles of the LSE. Nevertheless, coupling energy can solve this problem effectively. Taking the EGM as an example, when the gas wholesale price is lower during 18:00-24:00 and 1:00-8:00, meaning the market demands for natural gas are lower, the LSE can choose to bulk buy gas to storage or convert it into other types of energy which is at peak. When the gas wholesale price is higher at 9:00-17:00, in order to supply large demand in gas market, the LSE can further the profit by choosing to discharge natural gas in storage tank or buy more electricity instead of natural gas and then convert the electricity into gas with P2G technology. Of course, the conversion amount of P2G is not only influenced by gas price, but also the electricity price. The electricity price trough during 18:00-24:00 and 1:00-8:00 causes that P2G converts electricity into natural gas.
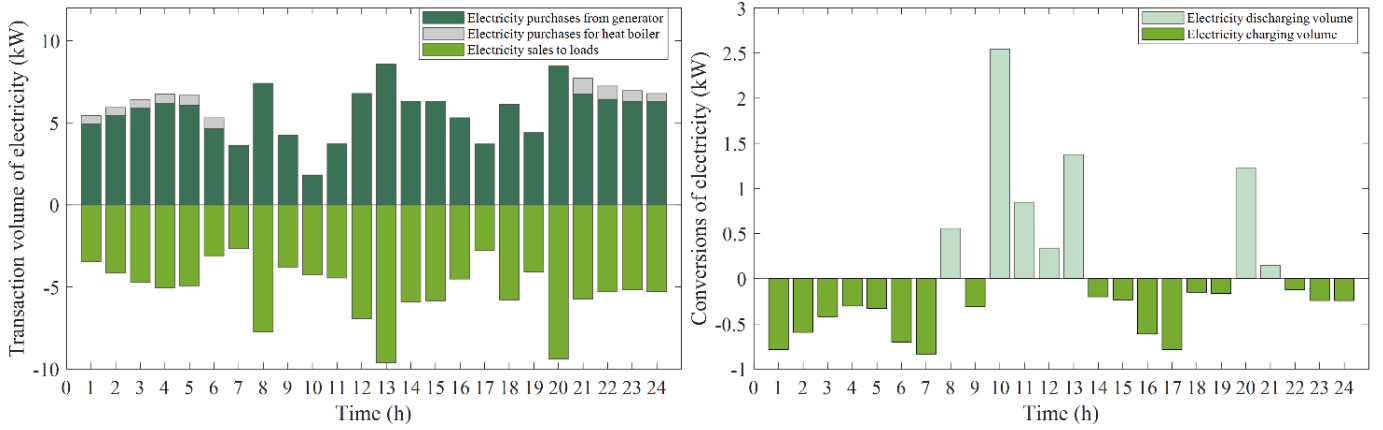

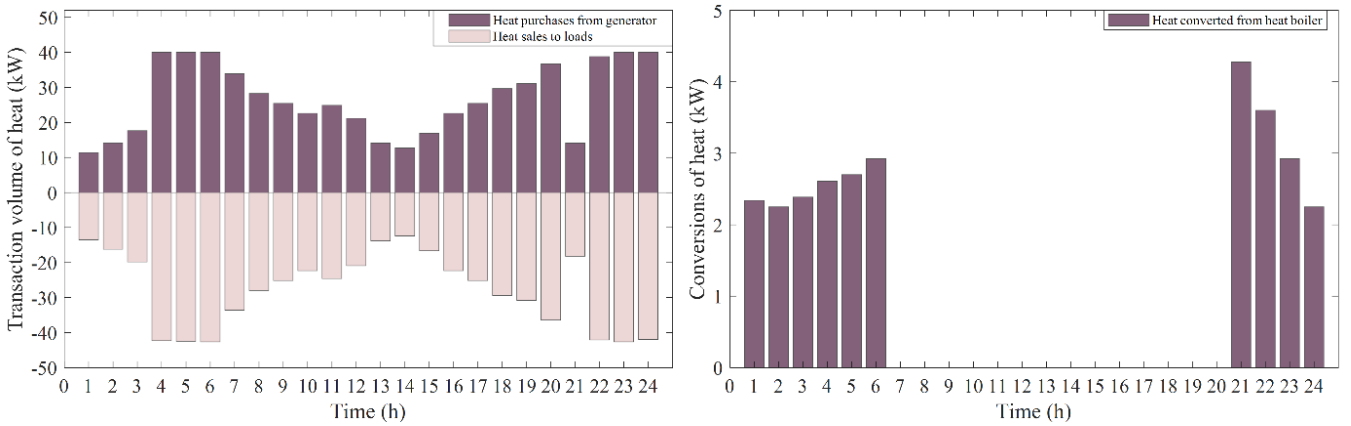(a) Electricity transaction and conversion during 24 hours
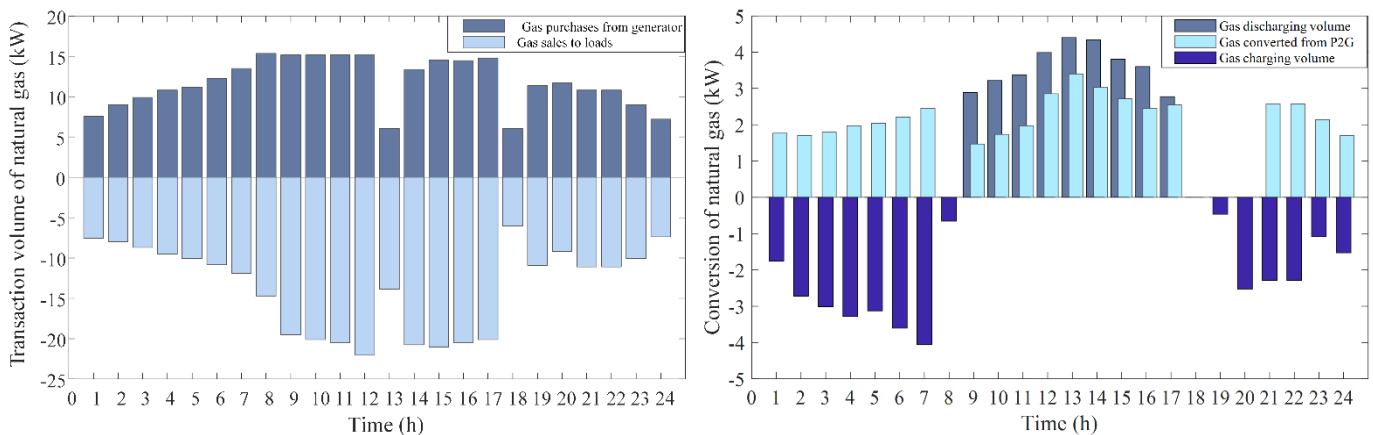
(b) Gas transaction and conversion during 24 hours

Fig. 11 Transaction and conversion results of the LSE in the EGM

22

(a) Electricity transaction and conversion during 24 hours

(b) Heat transaction and conversion during 24 hours

Fig. 12 Transaction and conversion results of the LSE in the EHM

If the LSE participates in the electricity market and gas market separately, the gross profit is $78.704, and the gas market is the most profit, followed by the power market and heat market, which can be obtained from Table II. While the gross profit in the EGM is $92.3294, which is an increase of 17.31% than isolated market. However, we can see that the profit of electricity trades in EGM is negative. As a typical profit-seeker, due to more profit in gas transaction, it is natural and reasonable for LSE to increase the trading volume of natural gas and decrease trading of electricity. Compared to the results in Fig. 10, the power demand curve is much flatter than those in the independent markets, but peak-valley difference of gas demand increases. The detail difference between the peak and valley is given in Table II.

In the electricity-heat market (EHM), an electric boiler combines heat with electricity to achieve energy interaction. The same situation can be observed in the EHM shown in Fig. 12. The profit increases by 6.04% comparing with isolated operation, and the electricity demand peak-valley difference value is dropped by 3.95%, while heat demand difference rises by 10.56%. Although heat boiler fill the heat demand valley at 1:00-6:00 and 21:00-24:00, both electricity market and heat market is in the valley period during 14:00-16:00, so it cannot not work during 14:00-16:00, the peak-valley difference of heat is still high.

4.3 Case C: Multi-energy market

In the multi-energy market proposed in this paper, the LSE is able to trade electricity, heat and natural gas simultaneously by responding to the respective market prices. Both the energy converters, including gas-fired CHPs, electric boilers and P2G systems, and storage devices make multi-energy transactions possible. The results of the energy transaction and conversion are plotted in Fig. 13. Energy transaction response to market prices of electricity, natural gas and heat correspondingly, while energy conversion rely on the EH.   Gas-fired CHP couples three types of energy together in this case via converting natural gas into electricity and heat. During 18:00-24:00 and 1:00-8:00, the LSE buys more natural gas thanks to lower price. Apart from basic gas demands, the LSE inputs excess natural gas into gas-fired CHP to satisfy power and heat market demands. For heat market especially, the LSE is at a loss during 1:00-4:00 in heat market, it's a certainly good strategy to obtain heat from gas-fired CHP instead of only trading in heat market. As a consequence, the large amount of heat conversion from CHP at 1:00-4:00 in Fig. 13(c) is reasonable. Obviously, the IDR in multi-energy market not only increases the diversity and flexibility of the trading means for the LSE, but also satisfy the requirement of the different types of end-users.

The gross profit in the multi-energy market is $164.1821, which has increased by 31.31 % compared with case A. This suggests that the more energy sources that participate in the multi-energy market, the more economic benefits and the better the IDR effect are. Therefore, it is necessary for both the LSE and loads to take part in the proposed multi-energy market.

Compared with the results in Fig. 10(a), Fig. 11(a) and Fig. 12(a), the complementation among the multiple energy peaks and valleys in this market leads to a much flatter electricity demand fluctuation. Compared with the results in case B, the difference values of electricity and natural gas demand are dropped by 4.98% and 12.48%, respectively. All things considered, for the LSE, IDR in multi-energy market increases the diversity and flexibility of market transaction leading more profit. For end-users, three types of energy can be satisfied better. For IES, loads fluctuation and peak-valley difference are decreased as a whole.
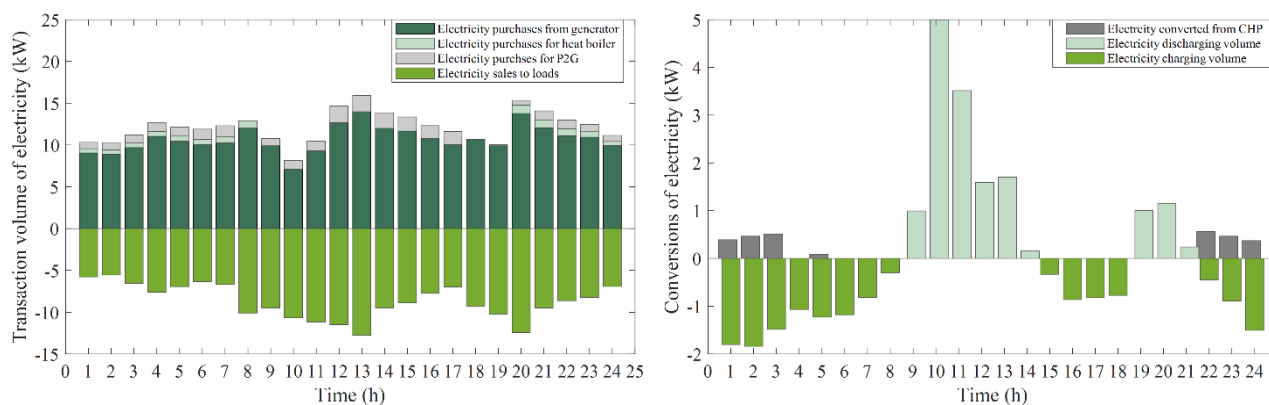
(a) Electricity transaction and conversion during 24 hours
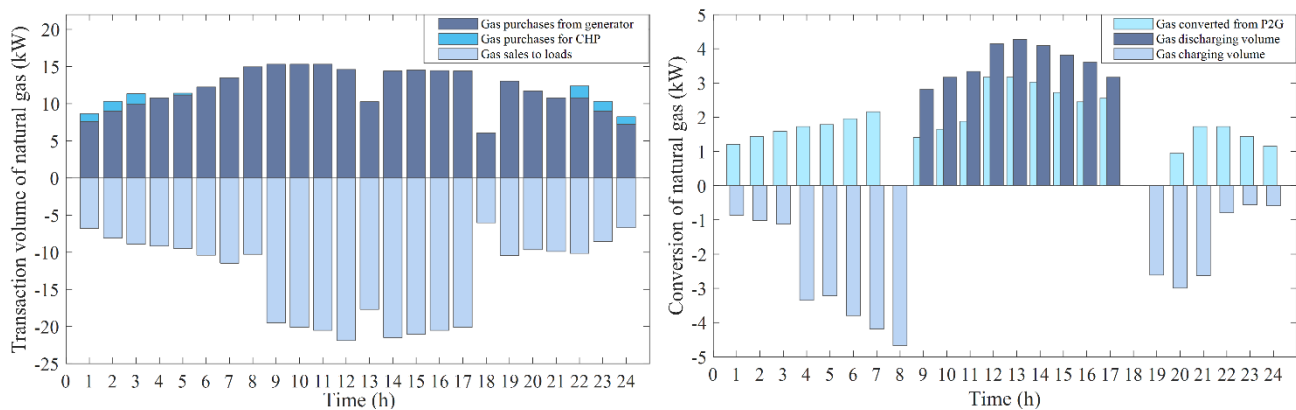
(b) Gas transaction and conversion during 24 hours
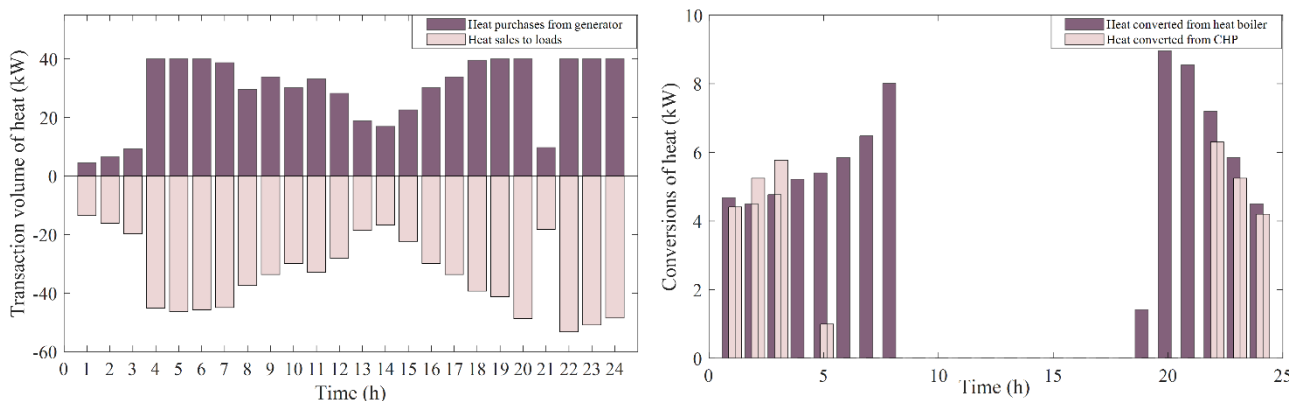
(c) Heat transaction and conversion during 24 hours

Fig. 13 Transaction and conversion results of LSE in multi-energy market

Table II The difference between the peak load and valley load

Market category	Electricity difference (kW)	Natural gas difference (kW)	Heat difference (kW)
Electricity market	6.3603	\	\
Natural gas market	\	12.9459	\
Heat market	\	\	27.3436
EGM	3.0065	16.0247	\
EHM	6.1092	\	30.2302
Multi-energy market (case C)	2.8568	14.0246	30.3181
Multi-energy market (case D)	5.9326	15.8668	39.7770

4.4 Case D: Analysis of the IES network constraints

The transaction of the multi-energy market is accompanied by the security operation of multi-energy flow networks. To verify the necessity of the IES network constraints for multi-energy market operation, focusing on the influence of the network operating variables, i.e., the voltage in a power system, gas pressure in a gas system, and temperature in a DHS, a comparative study was conducted in this case. The optimal results in case C are based on the IDR constraints in multi-energy market and voltage constraints, gas pressure constraints, and temperature constraints in the IES network. In case D, the optimal transaction strategy for the LSE will be discussed when the constraints on voltage, gas pressure, and temperature are ignored.

(1) Power distribution network

Fig. 14 presents the voltage profile of power distribution network in IES. It can be seen that several nodes voltages are less than the lower limit, i.e. 0.95 p.u., if the operation constrains are ignored. Taking the node voltage profile at 8:00 as an example, which is shown on the left in Fig. 14, only the voltages of nodes 1, 2, 3, 4, 19 and 20 in case D are between 0.95-1.05, all the rest of nodes are less than 0.95. In additional, compared with case C, the voltage of bus 31 in case D is less than the lower limit 0.95 p.u. when power demand is at trough period during 1:00-8:00, 11:00-18:00 and 20:00-24:00.
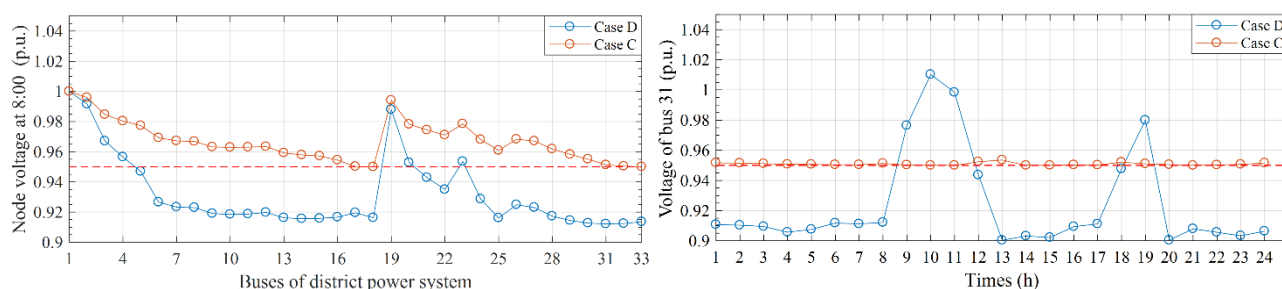

Fig. 14 Voltage profile in power system

(2) Natural gas network

In Fig. 15, the pressure of node 11 in case D is less than the lower bound of 10 mbar when gas transaction is at peak time during 8:00-10:00. Moreover, at 10:00, the pressure of 11 decreases to zero if the gas network operation constraint is ignored, which is not allowed obviously.
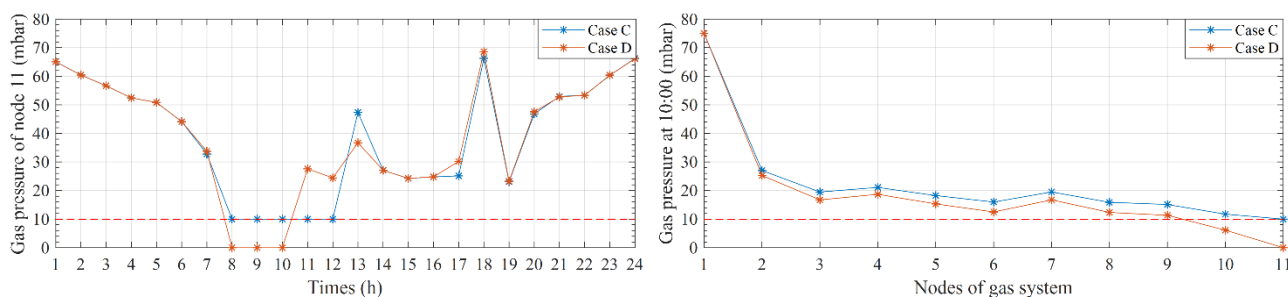
Fig. 15 Gas pressure profile in gas system

(3) District heating system

The supply temperature and return temperature of the DHS is shown in Fig. 16. The temperature is a key factor during the DHS operation, which is related to the heat flow in the pipeline. If the temperature is out of control, the mass flow in pipeline and heat balance will change accordingly. It can be observed in Fig.15 that there are large drops on both supply and return temperature in case D. Equation (46) and (48) indicate the heat input and output in DHS depends on the difference between supply temperature and return temperature at its node. The overall fall of temperature affect the temperature difference, which will further has influence on heat trading volume in the market. Hence, compared with the profit in case C, there is an obvious growth in the profit from the heat trading, $95.3664.

(a) Supply temperature of DHS

(b) Return temperature of DHS

Fig. 16 Temperature profile of DHS

The comparison above shows that voltage, gas pressure, and temperature of IES will be easily out of limit at peak period. Although the gross profit in case D increases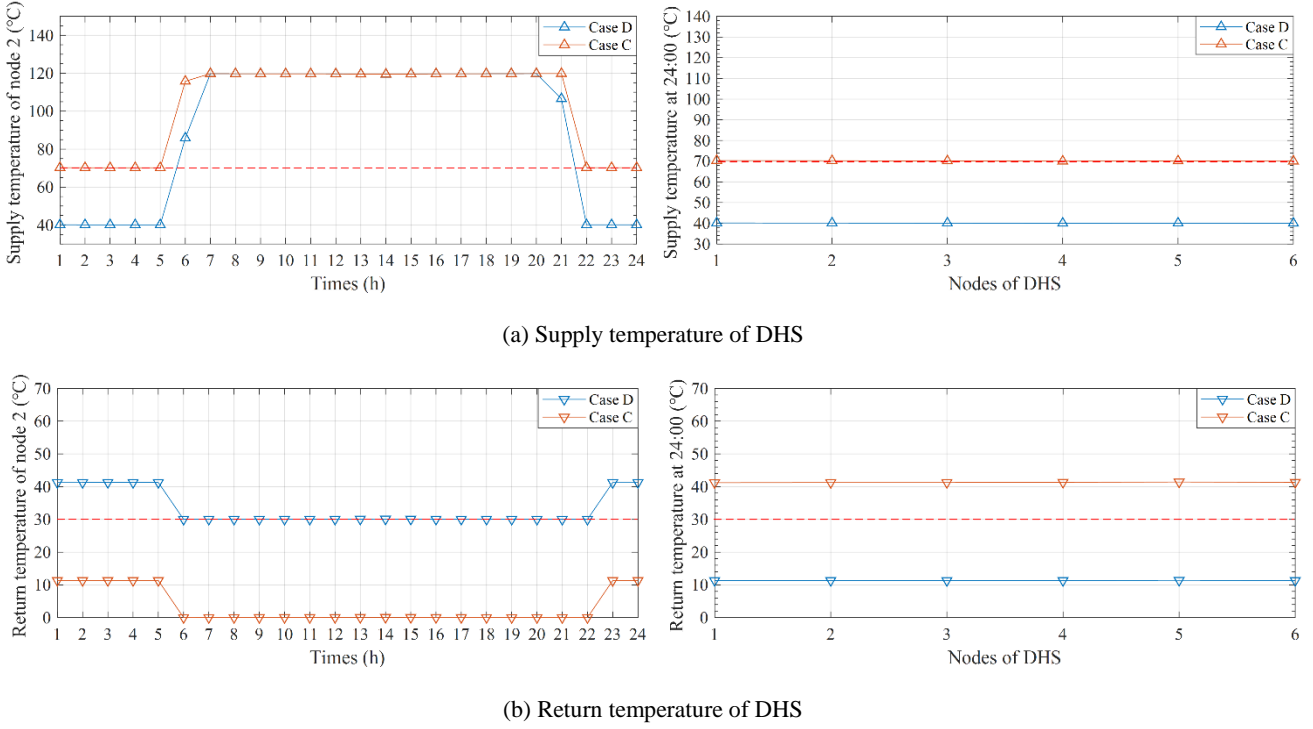 to \$176.0549, higher than that in case C, it is still not feasible to obtain optimal solution by only analyzing the market trading strategy while ignoring the IES network constraints. Thus, the execution of market transactions must satisfy security network constraints. To ensure the operation of a multi-energy market and network, it is crucial to maintain the balance between the economy and security.

5. Conclusions

The structure and mechanism of the multi-energy market are presented, and an optimal transaction strategy model of the load serving entity based on the integrated demand response (IDR) considering IES network constraints has been comprehensively studied. Considering multiple energy price signals, the goal of the IDR is to improve the profit of the LSE and make the multiple energy demand curves flatter. A set of tests are carried out on an IEEE 33-bus power system coupled with an 11-node gas system and a 6-node heat system test IES. The simulation results show that the LSE can achieve a higher profit by implementing an IDR in the multi-energy market. The IDR can improve the flexibility of the LSE in market participation. Furthermore, it offers guidelines to the end-users' market through price leverage and further reduces the load fluctuations. Moreover, a comparative study verifies the necessity for the IES to maintain the balance between the market economy and network security operation.

Appendix

The storage characteristics of storage battery in power systems:

$$ES_t = ES_{t-1} + E_{c,t}\zeta_E - E_{dc,t}/\zeta_E, \quad \forall t \in T \tag{A1}$$

$$\sum_{t=1}^{T} E_{c,t} = \sum_{t=1}^{T} E_{dc,t} \tag{A2}$$

$$ES_{\min} \le ES_t \le ES_{\min}, \quad \forall t \in T \tag{A3}$$

$$E_{c,\min} \le E_{c,t} \le E_{c,\min}, \quad \forall t \in T \tag{A4}$$

$$E_{dc,\min} \le E_{dc,t} \le E_{dc,\min}, \quad \forall t \in T \tag{A5}$$

Table AI Parameter setting in district power system

Bus	Voltage (p.u.)	Branch	From-to	Resistance	Reactance	Current
1	1	1	1-2	0.0922	0.0470	[0,100]
2	[0.95,1.05]	2	2-3	0.3930	0.2511	[0,100]
3	[0.95,1.05]	3	3-4	0.3660	0.1864	[0,100]
4	[0.95,1.05]	4	4-5	0.3811	0.1941	[0,100]
5	[0.95,1.05]	5	5-6	0.8190	0.7070	[0,100]
6	[0.95,1.05]	6	6-7	0.1872	0.6188	[0,100]
7	[0.95,1.05]	7	7-8	0.7114	0.2351	[0,100]
8	[0.95,1.05]	8	8-9	1.0300	0.7400	[0,100]
9	[0.95,1.05]	9	9-10	1.0440	0.7400	[0,100]
10	[0.95,1.05]	10	10-11	0.1966	0.0650	[0,100]
11	[0.95,1.05]	11	11-12	0.3744	0.1238	[0,100]
12	[0.95,1.05]	12	12-13	1.4680	1.1550	[0,100]
13	[0.95,1.05]	13	13-14	0.5416	0.7129	[0,100]
14	[0.95,1.05]	14	14-15	0.5910	0.5260	[0,100]
15	[0.95,1.05]	15	15-16	0.7463	0.5450	[0,100]
16	[0.95,1.05]	16	16-17	1.2890	1.7210	[0,100]
17	[0.95,1.05]	17	17-18	0.3720	0.5740	[0,100]
18	[0.95,1.05]	18	2-19	0.1140	0.1565	[0,100]
19	[0.95,1.05]	19	19-20	1.3042	1.3554	[0,100]
20	[0.95,1.05]	20	20-21	0.4095	0.4781	[0,100]
21	[0.95,1.05]	21	21-22	0.7089	0.9373	[0,100]
22	[0.95,1.05]	22	3-23	0.4512	0.3083	[0,100]
23	[0.95,1.05]	23	23-24	0.8980	0.7091	[0,100]
24	[0.95,1.05]	24	24-25	0.8960	0.7011	[0,100]
25	[0.95,1.05]	25	6-26	0.2030	0.1034	[0,100]
26	[0.95,1.05]	26	26-27	0.2842	0.1447	[0,100]
27	[0.95,1.05]	27	27-28	1.0590	0.9337	[0,100]
28	[0.95,1.05]	28	28-29	0.8042	0.7006	[0,100]
29	[0.95,1.05]	29	29-30	0.5075	0.2585	[0,100]
30	[0.95,1.05]	30	30-31	0.9744	0.9630	[0,100]

31	[0.95,1.05]	31	31-32	0.3105	0.3619	[0,100]
32	[0.95,1.05]	32	32-33	0.3410	0.5362	[0,100]
33	[0.95,1.05]	33	8-21	2.0000	2.0000	[0,100]
		34	9-15	2.0000	2.0000	[0,100]
		35	12-22	2.0000	2.0000	[0,100]
		36	18-33	0.5000	0.5000	[0,100]
		37	25-29	0.5000	0.5000	[0,100]

Table A Ⅱ Parameter setting in natural gas system

Node number	Pressure(mbar)	Pipeline number	From-to	Pipe length(m)	Pipe diameter(mm)
1	75	1	1-2	50	160
2	[10,75]	2	2-3	500	160
3	[10,75]	3	2-4	500	110
4	[10,75]	4	2-5	500	110
5	[10,75]	5	3-6	600	110
6	[10,75]	6	3-7	600	110
7	[10,75]	7	3-8	500	110
8	[10,75]	8	5-6	600	80
9	[10,75]	9	4-7	600	80
10	[10,75]	10	6-8	780	80
11	[10,75]	11	7-8	780	80
		12	7-9	200	80
		13	9-10	200	80
		14	10-11	200	80

Table A Ⅲ Parameter setting in DHS

Node number	Supply temperature(℃)	Return temperature(℃)	Pipeline number	From-to	Mass flow
1	[70,120]	[30,70]	1	1-2	75
2	[70,120]	[30,70]	2	2-3	50
3	[70,120]	[30,70]	3	3-4	25
4	[70,120]	[30,70]	4	2-5	25
5	[70,120]	[30,70]	5	3-6	25
6	[70,120]	[30,70]	\	\	\

References

[1]   W. L. Ahlgren, The Dual-Fuel Strategy: An Energy Transition Plan. Proceedings of the IEEE, vol. 100, no. 11, pp. 3001-3052, 2012.

[2]   World Energy Outlook 2013 Factsheet: How will global energy markets evolve to 2035, 2013.

[3]   T. Ding, Y. Xu, Y. Yang, Z. Li, X. Zhang, and F. Blaabjerg. A tight A Tight Linear Program for Feasibility Check and Solutions to Natural Gas Flow Equations. IEEE Transactions on Power Systems, 2019 (Early Access).

[4] K. Wang, X. Hu, H. Li, P. Li, D. Zeng, and S. Guo. A Survey on Energy Internet Communications for Sustainability. IEEE Transactions on Sustainable Computing, vol. 2, no. 3, pp. 231-254, 2017.

[5] Y. Hu, Z. Bie, T. Ding, and Y. Lin. An NSGA-II based multi-objective optimization for combined gas and electricity network expansion planning. Applied Energy, vol. 167, pp. 280-293, 2016.

[6] T. Ding, Y. Hu, and Z. Bie. Multi-Stage Stochastic Programming With Nonanticipativity Constraints for Expansion of Combined Power and Natural Gas Systems. IEEE Transactions on Power Systems, vol. 33, no. 1, pp. 317-328, 2018.

[7] M. A. Hannan, M. Faisal, P. J. Ker, and F. Blaabjerg. A Review of Internet of Energy Based Building Energy Management Systems: Issues and Recommendations. IEEE Access, pp. (99):1-1, 2018.

[8] V. Smith, and L. Kiesling. A Market-Based Model for ISO-Sponsored Demand Response Programs. 2005.

[9] S. Borenstein, J. B. Bushnell, and F. A. Wolak. Measuring Market Inefficiencies in California's Restructured Wholesale Electricity Market. American Economic Review, vol. 92, no. 5, pp. 1376-1405, 2002.

[10] J. Nicolaisen, V. Petrov, and L. Tesfatsion. Market power and efficiency in a computationale electricity market with discriminatory double-auction pricing. IEEE Trans.evol.comput, vol. 5, pp. 504-523, 2001.

[11] X. Fang, F. Li, Y. Wei, and H. Cui. Strategic scheduling of energy storage for load serving entities in locational marginal pricing market. IET Generation Transmission & Distribution, vol. 20, no.5, pp. 1258-1267, 2016.

[12] H. Li, and L. Tesfatsion. ISO Net Surplus Collection and Allocation in Wholesale Power Markets Under LMP. IEEE Transactions on Power Systems, vol. 26, no. 2, pp. 627-641, 2011

[13] H. Xu, K. Zhang, and J. Zhang. Optimal Joint Bidding and Pricing of Profit-seeking Load Serving Entity. IEEE Transactions on Power Systems, pp. (99):1-1, 2018.

[14] J. Lv, T. Ding, Z. Bie, P. Qin, T. Chen, and R. Liu. The design and optimization of the urban residential electricity packages for a load serving entity, Power and Energy Engineering Conference IEEE, pp. 69-73, 2016.

[15] H. Zhong, L. Xie, and Q. Xia. Coupon Incentive-Based Demand Response: Theory and Case Study. IEEE Transactions on Power Systems, vol. 28, no.2, pp. 1266-1276, 2013.

[16] X. Fang, Q. Hu, F. Li, B. Wang, and Y. Li. Coupon-Based Demand Response Considering Wind Power Uncertainty: A Strategic Bidding Model for Load Serving Entities. IEEE Transactions on Power Systems, vol. 31, no .2, pp. 1025-1037, 2016.

[17] A. Ghasemi, S. S. Mortazavi, and E. Mashhour. Integration of nodal hourly pricing in day-ahead SDC (smart distribution company) optimization framework to effectively activate demand response. Energy, vol. 86, pp. 649-660, 2015.

[18] S. M. de Oca, P. Belzarena, and P. Monzón. Benefits of optimal demand response in distribution networks in a competitive retail market. URUCON IEEE, pp. 1-4, 2017.

[19] S. Fan, Q. Ai, and L. Piao. Bargaining-based cooperative energy trading for distribution company and demand response. Applied Energy, vol. 226, pp. 469-482, 2018.

[20] S. Maharjan, Q. Zhu, Y. Zhang, S. Gjessing, and T. Başar. Dependable Demand Response Management in the Smart Grid: A Stackelberg Game Approach. IEEE Transactions on Smart Grid, vol. 4, no. 1, pp. 120-132, 2013.

[21] M. Rahmani-Andebili. Nonlinear demand response programs for residential customers with nonlinear behavioral models, Energy and Buildings, vol. 119, pp. 352-362, 2016.

[22] M. Rahmani-Andebili. Modeling nonlinear incentive-based and price-based demand response programs and implementing on real power markets, Electric Power System Research, vol. 132, pp. 115-124, 2016.

[23] M. Rahmani-Andebili, and H. Shen. Energy Management of End Users Modeling their Reaction from a GENCO's Point of View, International Conference on Computing, Networking and Communications (ICNC), Silicon Valley, USA, January 26-29, 2017.

[24] M. Rahmani-Andebili. Risk-Cost Based Generation Scheduling Smartly Mixed with Reliability and Market-Driven Demand Response Measures, International Transactions on Electrical Energy Systems, vol. 25, pp. 994-1007, 2015.

[25] Z. Li, W. Wu, M. Shahidehpour, J. Wang, and B. Zhang. Combined Heat and Power Dispatch Considering Pipeline Energy Storage of District Heating Network. IEEE Transactions on Sustainable Energy, vol. 7, no.1, pp.12-22, 2015.

[26] J. Zheng, J. Chen, Q. Wu, and Z. Jing. Multi-objective optimization and decision making for power dispatch of a large-scale integrated energy system with distributed DHCs embedded. Applied Energy, vol. 154, pp. 369-379, 2015.

[27] G. Li, R. Zhang, T. Jiang, H. Chen, L. Bai, H. Cui, and X. Li. Optimal dispatch strategy for integrated energy systems with CCHP and wind power. Applied Energy, vol. 192, 2016.

[28] J. Li, J. Fang, Q. Zeng, and Z. Chen. Optimal operation of the integrated electrical and heating systems to accommodate the intermittent renewable sources. Applied Energy, vol. 167, pp. 244-254, 2016.

[29] Y. Cheng, N. Zhang, and C. Kang. Low-carbon economic dispatch for integrated heat and power systems considering network constraints. The Journal of Engineering, vol. 2017, no. 14, pp. 2628-2633, 2017.

[30] C. R. Touretzky, D. L. Mcguffin, J. C. Ziesmer, and M. Baldea. The effect of distributed electricity generation using natural gas on the electric and natural gas grids. Applied Energy, vol. 177, pp. 500-514, 2016.

[31] Q. Zeng, J. Fang, J. Li, and Z. Chen. Steady-state analysis of the integrated natural gas and electric power system with bi-directional energy conversion. Applied Energy, 2016.

[32] F. Liu, Z. Bie, and X. Wang. Day-Ahead Dispatch of Integrated Electricity and Natural Gas System Considering Reserve Scheduling and Renewable Uncertainties. IEEE Transactions on Sustainable Energy, pp. (99):1-1, 2018.

[33] L. Bai, F. Li, H. Cui, T. Jiang, H. Sun, and J. Zhu. Interval optimization based operating strategy for gas-electricity integrated energy systems considering demand response and wind uncertainty. Applied Energy, vol. 167, pp. 270-279, 2016.

[34] S. Bahrami, and A. Sheikhi. From Demand Response in Smart Grid Toward Integrated Demand Response in Smart Energy Hub. IEEE Transactions on Smart Grid, vol. 7, no. 2, pp. 650-658, 2016.

[35] M. C. Bozchalui, S. A. Hashmi, H. Hassen, C. A. Cañizares, and K. Bhattacharya . Optimal Operation of Residential Energy Hubs in Smart Grids. IEEE Transactions on Smart Grid, vol. 3, no. 4, pp. 1755-1766, 2012.

[36] E. A. Martinez Cesena, and P. Mancarella. Energy Systems Integration in Smart Districts: Robust Optimisation of Multi-Energy Flows in Integrated Electricity, Heat and Gas Networks. IEEE Transactions on Smart Grid, pp. (99):1-1, 2018.

[37] A. Sheikhi, M. Rayati, S. Bahrami, and A. M. Ranjbar. Integrated Demand Side Management Game in Smart Energy Hubs. IEEE Transactions on Smart Grid, vol. 6, no. 2, pp. 675-683, 2015.

[38] L. Ye, B. Peng, J. Hao, and Y. Zhang. The coordinated operation scheduling of distributed generation, demand response and storage based on the optimization energy hub for minimal energy usage costs. International Conference on Power and Renewable Energy, pp. 649-653, 2017.

[39] M. Rastegar, M. Fotuhi-Firuzabad, H. Zareipour, and M. Moeini-Aghtaie. A Probabilistic Energy Management Scheme for Renewable-Based Residential Energy Hubs. IEEE Transactions on Smart Grid, vol. 8, no. 5, pp. 2217-2227, 2017.

[40] M. Alipour, K. Zare, and M. Abapour. MINLP Probabilistic Scheduling Model for Demand Response Programs Integrated Energy Hubs. IEEE Transactions on Industrial Informatics, pp. (99):1-1, 2017.

[41] M. Moeini-Aghtaie, P. Dehghanian, M. Fotuhi-Firuzabad, and A. Abbaspour. Multiagent Genetic Algorithm: An Online Probabilistic View on Economic Dispatch of Energy Hubs Constrained by Wind Availability. IEEE Transactions on Sustainable Energy, vol. 5, no. 2, pp. 699-708, 2014.

[42] Q. Jia, Y. Yang, L. Xia, X. Guan. A Tutorial on Event-Based Optimization with Application in Energy Internet. Control Theory & Applications, 2018.

[43] F. Song, X. Guan, J. Wu, D. Xie, W. Liu, and L. Chen. Particle filter based on partial accurate observation for high dimensional stochastic dynamic system, pp. 4604-4609, 2017.

[44] J. Dong, F. Gao, X. Guan, Q. Zhai, and J. Wu. Storage Sizing with Peak-shaving Policy for Wind Farm Based on Cyclic Markov Chain Model. IEEE Transactions on Sustainable Energy, pp. (99):1-1, 2018.

[45] D, Wang, D, Kalathil, K, Poolla, and X. Guan. Coordination of wind power and flexible load through demand response options. IEEE Conference on Decision and Control. IEEE, pp. 7226-7231, 2015.

[46] J. Wu, J. Yan, H. Jia, N. Hatziargyriou, N. Djilali, and H. Sun. Integrated Energy Systems. Applied Energy, vol. 167, pp. 155-157,

2016.

[47] X. Jin, Y. Mu, H. Jia, J. Wu, X. Xu, and X. Yu. Optimal day-ahead scheduling of integrated urban energy systems. Applied Energy, vol. 180, pp. 1-13, 2016.

[48] X. Liu, and P. Mancarella. Modelling, assessment and Sankey diagrams of integrated electricity-heat-gas networks in multi-vector district energy systems. Applied Energy, vol. 167, pp. 336-352, 2016.

[49] W. Gu, J. Wang, S. Lu, Z. Luo, and C. Wu. Optimal operation for integrated energy system considering thermal inertia of district heating network and buildings. Applied Energy, vol. 199, pp. 234-246, 2017.

[50] J. Wang, H. Zhong, Z. Ma, Q. Xia, and C. Kang. Review and prospect of integrated demand response in the multi-energy system. Applied Energy, vol. 202, 2017.

[51] M. Pirouti. Modelling and analysis of a district heating network. Cardiff University, 2013.

[52] M. Abeysekera, J. Wu, N. Jenkins, and M. Rees. Steady state analysis of gas networks with distributed injection of alternative gas. Applied Energy, vol. 164, pp. 991-1002, 2016.

[53] M. Salahi, F. Mehrdoust, and F. Piri. CVaR Robust Mean-CVaR Portfolio Optimization. Isrn Applied Mathematics, vol. 2013, no. 2013, pp. 73-81, 2014.